

6-2022

## Analysis of COVID-19 and Vaccine Administration in Mississippi

Megan Sickinger

*The University of Southern Mississippi*

Follow this and additional works at: [https://aquila.usm.edu/honors\\_theses](https://aquila.usm.edu/honors_theses)



Part of the [Ordinary Differential Equations and Applied Dynamics Commons](#)

---

### Recommended Citation

Sickinger, Megan, "Analysis of COVID-19 and Vaccine Administration in Mississippi" (2022). *Honors Theses*. 860.

[https://aquila.usm.edu/honors\\_theses/860](https://aquila.usm.edu/honors_theses/860)

This Honors College Thesis is brought to you for free and open access by the Honors College at The Aquila Digital Community. It has been accepted for inclusion in Honors Theses by an authorized administrator of The Aquila Digital Community. For more information, please contact [Joshua.Cromwell@usm.edu](mailto:Joshua.Cromwell@usm.edu).

Analysis of COVID-19 and Vaccine Administration in Mississippi

by

Megan Sickinger

A Thesis  
Submitted to the Honors College of  
The University of Southern Mississippi  
in Partial Fulfillment  
of Honors Requirements

May 2022



Approved by:

---

Zhifu Xie, Ph.D.,  
Thesis Advisor,  
School of Mathematics and Natural Sciences

---

Bernd Schroeder, Ph.D.,  
Director,  
School of Mathematics and Natural Sciences

---

Sabine Heinhorst, Ph.D.,  
Dean,  
Honors College

## ABSTRACT

In this work, we develop a simple mathematical model to observe the spread of COVID-19 and vaccine administration in Mississippi. Based on the well-known Kermack-McKendrick Susceptible-Infected-Removed epidemiological model, the *ASIRD – V* model has eight ordinary differential equations that split infected populations and recovered populations into vaccinated and unvaccinated populations. After determining that the system is reliable for real-world applications, we investigate and determine the stability and equilibrium points of this system. The system is found to be disease-free when  $\mathcal{R}_0 < 1$  and endemic when  $\mathcal{R}_0 > 1$ . We use MATLAB to numerically solve the system and optimize the model's parameters over four short periods, two with the presence of vaccines and two without the presence of vaccines, using death data and vaccine data given by the Centers for Disease Control. By calculating the reproduction numbers of the time periods, we analyze the effects of certain policy changes as well as the reliability of this model in predicting the spread of the disease. While the health policies at the start of the pandemic are reliable short-term solutions to slow the spread, the presence of fully vaccinated individuals slows the spread in the long term.

**Keywords:** COVID-19, ASIRD-V model, Stability, Parameter optimization, Vaccinations, Reproduction number, Numerical simulation

## ACKNOWLEDGMENTS

I would like to acknowledge the board and donators of the Wright. W and Annie Rea Cross Mathematics Undergraduate Research Scholarship for their support in this research. Without their funding, this research would not be possible. I would also like to acknowledge Anthony Panella and his work with the ASIRD model. Finally, I would like to acknowledge my Honors Thesis advisor Dr. Zhifu Xie, who has been a great help to me in my research.

## TABLE OF CONTENTS

|  |      |
|--|------|
| LIST OF ILLUSTRATIONS . . . . .          | vii  |
| LIST OF ABBREVIATIONS . . . . .          | viii |
| CHAPTER I: INTRODUCTION . . . . .        | 1    |
| CHAPTER II: LITERATURE REVIEW . . . . .  | 3    |
| CHAPTER III: METHODOLOGY . . . . .       | 8    |
| ASIRD-V Model . . . . .                  | 9    |
| Equilibrium Analysis . . . . .           | 10   |
| Reproduction Number . . . . .            | 13   |
| Linear Stability Analysis . . . . .      | 15   |
| CHAPTER IV: RESULTS . . . . .            | 19   |
| Without Vaccine Administration . . . . . | 19   |
| With Vaccine Administration . . . . .    | 26   |
| CHAPTER V: CONCLUSION . . . . .          | 37   |
| Future Research . . . . .                | 40   |
| APPENDIX A: Code . . . . .               | 42   |
| APPENDIX B: Data . . . . .               | 45   |
| REFERENCES . . . . .                     | 48   |

## LIST OF ILLUSTRATIONS

|    |   |    |
|----|---|----|
| 1  | Schematic for ASIRD-V Model . . . . .                                       | 9  |
| 2  | Solution of Susceptible Population from March 4 to March 26, 2020 . . . . . | 21 |
| 3  | $I, A_u, A_v, R_u, R_v, D$ from March 4 to March 26, 2020 . . . . .         | 21 |
| 4  | Data fitting for $D$ from March 4 to March 23, 2020 . . . . .               | 22 |
| 5  | $S$ from March 23 to April 4, 2020 . . . . .                                | 24 |
| 6  | $I, A_u, A_v, R_u, R_v, D$ from March 23 to April 4, 2020 . . . . .         | 25 |
| 7  | Data fitting for $D$ , from March 23 to April 1, 2020 . . . . .             | 25 |
| 8  | Data fitting for $D$ , from December 16 to December 22, 2020 . . . . .      | 28 |
| 9  | Data fitting for $V$ from December 16 to December 22, 2020 . . . . .        | 28 |
| 10 | $S$ from December 16 to December 22, 2020 . . . . .                         | 29 |
| 11 | $I$ and $A_u$ from December 16 to December 22, 2020. . . . .                | 29 |
| 12 | $R_u$ , December 16 to December 22, 2020 . . . . .                          | 30 |
| 13 | $A_v$ from December 16 to December 22, 2020 . . . . .                       | 30 |
| 14 | $R_v$ from December 16 to December 22, 2020 . . . . .                       | 31 |
| 15 | $S$ from March 6 to March 24, 2021 . . . . .                                | 33 |
| 16 | $I$ and $A_u$ from March 6 to March 24, 2021 . . . . .                      | 33 |
| 17 | $R_u$ from March 6 to March 24, 2021 . . . . .                              | 34 |
| 18 | $A_v$ from March 6 to March 24, 2021 . . . . .                              | 34 |
| 19 | $R_v$ from March 6 to March 24, 2021 . . . . .                              | 35 |
| 20 | Data fitting $V$ from March 6 to March 24, 2021 . . . . .                   | 35 |
| 21 | Data fitting for $D$ from March 6 to March 24, 2021 . . . . .               | 36 |



## LIST OF ABBREVIATIONS

|      |  |
|------|--|
| ARDS | Acute Respiratory Distress Syndrome      |
| CDC  | Centers for Disease Control              |
| MDHS | Mississippi Department of Human Services |
| MS   | Mississippi                              |
| WHO  | World Health Organization                |

## CHAPTER I: INTRODUCTION

In December of 2019, Severe Acute Respiratory Coronavirus 2 (SARS-CoV-2), which is known to cause COVID-19, was discovered in many patients battling pneumonia in Wuhan, China. By spreading through airborne particles and infected surfaces, COVID-19 traveled throughout the world, and the World Health Organization (WHO) declared this epidemic an international health emergency by January 30, 2020. This disease spreads through the air and surfaces much like the influenza viruses, although the coronavirus is much more infectious. In addition, influenza viruses have preventative vaccines, so COVID-19 spread comparatively faster without that control measure. By March 6, 2020, the first case of COVID-19 appeared in Mississippi, and by March 11 the WHO declared COVID-19 a pandemic, giving rise to the "new normal" as we live with the virus today.

Symptoms of COVID-19 appear approximately between 2 to 14 days after exposure and can range from asymptomatic to severe. Symptoms commonly include fever, chills, cough, shortness of breath or difficulty breathing, loss of taste and smell, and nausea. While most people only acquire mild symptoms, others such as the elderly and those with certain underlying health problems are at greater risk of contracting severe symptoms. While treatments for mild symptoms include fever reducers and rest, more severe symptoms could land an individual in the hospital. The case fatality rate in the United States began at approximately 2%, and the case fatality rate fluctuated as the coronavirus spread during the pandemic [26]. COVID-19 is known to cause an inflammation of the lungs known as Acute Respiratory Distress Syndrome (ARDS), and this requires a ventilator for assistance in fighting the disease. Many other complications have been known to arise from COVID-19, and the severity of these complications can be deadly. Following health guidelines determined by the World Health Organization and the Centers for Disease Control (CDC) is crucial to prevent more deaths from occurring in the United States of America.

Without a vaccine for COVID-19, preventative measures had to consist solely of quarantine, social distancing, increased hygiene, masks, and isolation. With guidance from

the CDC and the Mississippi Department of Human Service (MDHS), Mississippi Governor Tate Reeves enacted several Executive Orders as preventative measures against this disease throughout the pandemic [22]. These included state- and county-wide mask mandates, the closing of schools and nonessential businesses for a short period, Safer-At-Home orders encouraging the population to maintain isolation, and social distancing without large gatherings. Meanwhile, pharmaceutical companies Pfizer and Moderna were rapidly developing the mRNA vaccines, finally releasing the first doses in Mississippi by December of 2020 [12]. The COVID-19 pandemic became a crisis as Mississippi officials, as well as United States officials, scrambled to find the best solutions to curbing the rate of infections. The field of epidemiology uses mathematical modeling to help these policymakers in their decisions.

For epidemiologists, COVID-19 opened new research to study the effects and spread of this new virus and predict its spread to inform health officials and policymakers. The research includes developing new mathematical models to understand how transmission occurs in a given population. The asymptomatic cases discovered in the pandemic spurred many model variations, some more complicated than others, and as more information about the disease was released, the more accurate these mathematical models could become. In addition, the mutation of COVID-19 into several variants has provided an opportunity to compare transmission rates and accuracy in different models. In this study, we have explored many of these models, and the complexity of many of these models provided accurate simulations and predictions. However, in this study we developed a simple model that accounts for asymptomatic cases as well as the eventual introduction of vaccine administrations in Mississippi.

## CHAPTER II: LITERATURE REVIEW

Many of these epidemiological models are based on basic variations of the Kermack and McKendrick Susceptible-Infected-Removed (*SIR*) model [1]. However, very few models included compartments for both asymptomatic cases and a vaccinated control measure. Many of these models varied widely in complexity and included several compartments to accurately simulate and predict the spread of COVID-19. Depending on what the researchers wanted to observe and understand, different parameters, compartments, and control mechanisms were added to these systems. In addition, some of these models were made to observe long, continuous time periods while others were made to observe short time periods in the pandemic.

In epidemiological models, the basic reproduction number,  $\mathcal{R}_0$ , is the expected number of secondary cases caused by one infected individual. This number is a threshold parameter that tells us whether a disease will sustain in a population or eventually die out. If  $\mathcal{R}_0 < 1$ , then eventually there will not be enough infected individuals to spread the disease, and the disease will stop spreading. If  $\mathcal{R}_0 > 1$ , then more people will become infected as time passes, and the disease will spread. The reproduction number of a model arises from theoretical analysis, and [6] presented the Next-Generation matrix method to derive the reproduction number based on the disease-free equilibrium of the system. The reproduction number of a system is crucial to analyzing the spread of diseases since it provides an indication of the infectiousness of a disease and quantifies it. Since the infectiousness of a disease depends on many factors, the reproduction number is not the same for all models and countries. The reproduction number can change throughout time, caused by outside factors such as health control measures and vaccine effectiveness.

This research is an extension of the 2021 Undergraduate Summer Cross Scholar Research Program at the University of Southern Mississippi. In the 2021 summer research program, a simple model was developed to analyze the beginning of the pandemic in Mississippi, the *ASIRD* model [16]. The literature reviewed for the *ASIRD* model was written at the beginning of the pandemic before and immediately after vaccines were

developed.

In 2021, Abdy et al. used a fuzzy parameter in their *SIR* model to reflect real-world problems such as uncertainty in testing [2]. In addition, by using the basic *SIR* model, they added parameters for vaccine effectiveness and treatment effectiveness in the removed compartment. The membership functions of the fuzzy parameters incorporated in the *SIR* model allowed for dependence on the capacity to carry the disease by an individual. Abdy et al. simulated the effects of vaccines, treatments, and infections by using data from Indonesia effectively [2]. We take away from this model the idea that measuring uncertainty in our model will be useful to gain an understanding of the effects of infections.

Krivorot'ko et al. studied the reliability of the *SEIR – D* and *SEIR – HCD* models and compared their simulation results to find the best fit and accurate simulation of the pandemic in Moscow and the Novosibirsk region [3]. In their research, the *SEIR – D* model created the most accurate simulations for the Novosibirsk region and the best historical approximation of cases and deaths in Moscow. In addition, the *SEIR – D* model had the smallest error in forecasting the longest period for Moscow [3]. Krivorot'ko et al. displayed the importance of available information to the reliability of a model. Without sufficient data available for the model to measure, a model will not be as effective in simulating or forecasting the spread of the disease. In our study, we wanted to utilize the data made available to us to create a reliable model.

Neves and Guerrero introduced a simple variation of the *SIR* model by adding an asymptomatic compartment and developed the *A – SIR* model to study the COVID-19 pandemic in Italy and Brazil [23]. By adding a compartment for asymptomatic individuals, the model accounted for the unpredictability of those who are positive with COVID-19 but not tested either due to the lack of testing or the lack of recognizable symptoms. From the literature above, the *ASIRD* model developed in the Cross Scholar Summer Research program is a variation of the models studied in the references [24] [23], where we wanted to observe the effects of the asymptomatic cases with the data on deceased individuals made available by MDHS and the CDC. Through the Cross Scholar Summer Research program,

we simulated the *ASIRD* model over the beginning of the pandemic and discovered the model most effectively simulated the pandemic for short periods of time. In the modification of the *ASIRD* model to include vaccinations, the following literature was reviewed.

Ramos et al. began with a simple but complex enough  $\theta - SIR$  type model in application to the COVID-19 pandemic in Italy [5]. The  $\theta - SEIHQRD$  model developed by Ramos et al. added all necessary complexities to a traditional *SIR* model that are important to helping policymakers, with data and research to support each parameter. Bachar et al. modeled the spread of COVID-19 and control mechanisms in Saudia Arabia using numerical simulations of their  $S_L S_M E I_U I_D R_u R_D E_x$  system for a short time [11]. The system of Bachar et al. split infected and recovered compartments into undiagnosed and diagnosed, an interesting take on the uncertainty of testing. Meanwhile, Hongfan et al. used a *SIQR* model with a time delay for COVID-19 to consider the impact of treatment time and its effect on the pandemic using numerical simulations [25]. In one research article, the basic reproduction number of COVID-19 is estimated in Ghana using an *SEIAHR* model and the next-generation matrix method, which we found helpful in finding the basic reproduction number for our system [15]. One study also included the complexity of adding the dynamics of another disease alongside COVID-19; although far too complex for an application to the population of Mississippi, it offered an interesting insight into the dynamics of different diseases within a pandemic [14].

In this study, we considered asymptomatic cases as an unpredictable but important factor to include in simulations and predictions. Since asymptomatic individuals can infect others with the disease without showing symptoms, including these individuals is important to understand how the disease spreads. Olivares et al. developed an *SEI<sub>s</sub>I<sub>a</sub>QR* model to quantify uncertainty under a mass vaccination strategy, where asymptomatic individuals were placed in the compartment  $I_a$  [9]. Aziz-Alaoui et al. introduced a simple yet effective *SIARD* model focused on non-total immunity while observing the death rate of asymptomatic individuals in a stochastic approach [24]. While the *SIARD* model is similar to the one we develop in this study, we did not consider the reinfection rate because of the

short time periods we observed.

Since the vaccine for COVID-19 was developed almost a year after the spread was declared a pandemic, many models did not include vaccine mechanisms or vaccinated compartments. However, once the administration of the vaccines began, researchers were able to include vaccine compartments and mechanisms in their models to observe the effect of different administration policies around the world. In another study, Ramos et al. refined their previous research and developed a  $\theta - ij - SVEIHQRD$  model for the impact of variants and vaccines on the pandemic in Italy [10]. By including a vaccination compartment, they were able to study the effectiveness of the vaccines against different COVID-19 variants. Although they did not include a separate compartment for a vaccinated population, De la Sen et al. used parameters to estimate vaccine and antiviral controls in their  $SEI_s I_h AR$  model [7]. In addition, Zhang et al. developed a discretized  $SIRVS$  model to study the permanence of a disease with vaccinations present [8]. While the  $SIRVS$  model was not in any particular application to the COVID-19 pandemic, it provided a useful basis for adding vaccination compartments into a system.

While not as simple as the  $A - SIR$  model, the model we developed includes a death compartment for more accurate optimization as well as a vaccine compartment to account for the vaccine control measures beginning farther into the pandemic. Based on the available data for Mississippi, we chose compartments for the vaccinated, asymptomatic, susceptible, infected, recovered, and deceased populations. Some of these compartments were split to observe the effect of possible breakthrough cases as vaccine efficacy decreased [17]. The  $ASIRD - V$  model was developed since we did not want to introduce compartments without having sufficient data to support an accurate simulation of the spread of the disease. The simplicity of the model takes the deceased data, vaccine data, and confirmed cases data of Mississippi as support for simulations made in this study. The vaccine efficacy for COVID-19 in certain time periods is also known and provided by the CDC [12] [13].

The next section of this study is the development of the  $ASIRD - V$  model for COVID-19 in Mississippi. In Chapter III, we developed the methodology for creating the

*ASIRD – V* model, conducted an equilibrium analysis, and proved the linear stability using the basic reproduction number of the system. In Chapter IV, we simulated the model numerically and showed results for short time spans at the beginning of the pandemic, in the time span during the first doses of administered vaccines, and in the time span for fully vaccinated, susceptible individuals. By comparing the reproduction number of each simulation, we observed the effect of vaccinations and other health policies on the pandemic in Mississippi. Finally, we deduced conclusions in Chapter V from the results in Chapter IV.



### CHAPTER III: METHODOLOGY

The Asymptomatic-Susceptible-Infected-Recovered-Deceased (*ASIRD*) model was altered to accommodate those who have been vaccinated against COVID-19 [16]. While this vaccination occurred, the disease began to spread widely, providing the chance for vaccine effectiveness to drop and cause breakthrough cases [19]. Since these breakthrough cases accounted for a significant part of the population, the vaccinated compartment was treated as a susceptible compartment, where those who were in the susceptible population may receive the vaccine with an immunity rate lower than 90% [20] [19]. In addition, some studies showed the predominance of the Delta variant decreased the effectiveness of two doses of the Pfizer or Moderna vaccines (mRNA) to only 66% among healthcare workers and as low as 53% among nursing home residents [17] [18]. Any breakthrough cases traveled to the vaccinated, asymptomatic compartment, where the vaccinated but infected could infect others. Those who are positive for COVID-19 but vaccinated experienced milder symptoms than those without the vaccine. To study the effect of this small population, the asymptomatic compartment was split to observe those with and without the vaccine and how these two populations recovered differently [19]. The recovered compartments contain those who have recovered from illness, so those who were immune because of the vaccine stayed in the vaccinated compartment since there was no logical reason to move them to the recovered compartment if they had never been infected.

## ASIRD-V Model

$$\begin{aligned}
 \frac{dS}{dt} &= -S(\alpha_I I + \alpha_A A_u + \alpha_A A_v) - \nu S \\
 \frac{dI}{dt} &= \xi S(\alpha_I I + \alpha_A A_u + \alpha_A A_v) - (\rho_s + \mu) I \\
 \frac{dA_u}{dt} &= (1 - \xi) S(\alpha_I I + \alpha_A A_u + \alpha_A A_v) - \rho_{au} A_u \\
 \frac{dA_v}{dt} &= (1 - \tau) V(\alpha_I I + \alpha_A A_u + \alpha_A A_v) - \rho_{av} A_v \\
 \frac{dR_u}{dt} &= \rho_s I + \rho_{au} A_u \\
 \frac{dR_v}{dt} &= \rho_{av} A_v \\
 \frac{dD}{dt} &= \mu I \\
 \frac{dV}{dt} &= \nu S - (1 - \tau) V(\alpha_I I + \alpha_A A_u + \alpha_A A_v)
 \end{aligned} \tag{1}$$

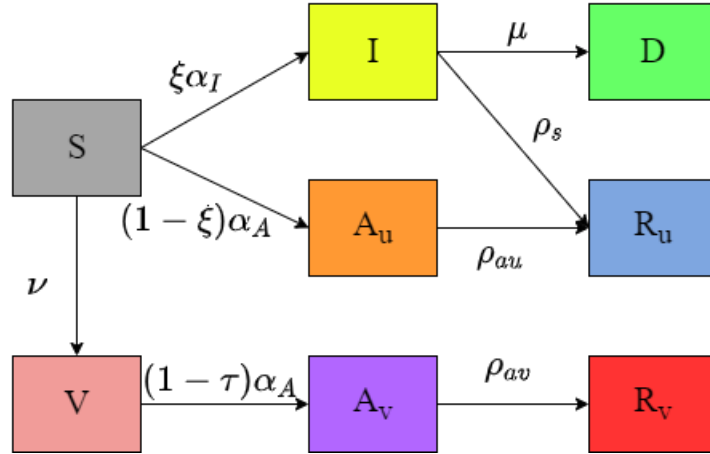


Figure 1: Schematic for ASIRD-V Model

The system of ordinary differential equations has nine parameters that move individuals from one compartment to the next. Each compartment is a population represented by an ordinary differential equation. We have the susceptible population  $S$ , which we assumed to be the entire population of Mississippi. Susceptible individuals are vaccinated at a rate of  $\nu$  or become infected at a rate of  $\alpha_I$  or  $\alpha_A$ . Since we are observing the pandemic for short periods of time, we assumed no reinfections occur from recovered individuals during each

time period. We also assumed that breakthrough cases could occur in the vaccinated population  $V$  since the vaccine efficacy  $\tau$  cannot represent total immunity to the disease. There is a probability of  $(1 - \tau)$  that a breakthrough case occurs, and vaccinated, susceptible individuals become infected at a rate of  $\alpha_A$ . Meanwhile, we have three infectious populations: the symptomatic infected  $I$ , the unvaccinated asymptomatic  $A_u$ , and the vaccinated asymptomatic  $A_v$ . There is a probability  $\xi$  that a susceptible individual develops symptoms, and a probability  $(1 - \xi)$  that a susceptible individual becomes asymptomatic. We assumed that both unvaccinated and vaccinated asymptomatic individuals have little to no symptoms with no testing and no hospitalization or death; symptomatic individuals have symptoms severe enough to be tested and quarantined, as well as possible hospitalization and death. However, we assumed that vaccinated and infected individuals recover differently at a rate of  $\rho_{av}$  than both unvaccinated symptomatic and asymptomatic individuals with a recovery rate of  $\rho_s$  or  $\rho_{au}$ , respectively. There are two recovered populations: the unvaccinated recovered  $R_u$  and the vaccinated recovered  $R_v$ . The symptomatically infected individuals transfer to the deceased population  $D$  at a death rate of  $\mu$ . Figure 1 shows the flow of individuals as parts of the susceptible population become vaccinated, infected, or both, and eventually recover or die. The infection rates of symptomatic and asymptomatic individuals are  $\alpha_I$  and  $\alpha_A$ , respectively, and  $\xi$  is the probability a case becomes symptomatic. The recovery rates for symptomatic and asymptomatic individuals without vaccines are  $\rho_s$  and  $\rho_{au}$  while the recovery rate for breakthrough cases is  $\rho_{av}$ . The death rate is described by the parameter  $\mu$ , where only those with severe symptoms in the infected population could die. The daily vaccination rate is described by the parameter  $\nu$  while the immunity rate of the vaccines is described by  $\tau$ . To show that this system can simulate the pandemic with reasonable results, we first proved that the solutions of the system are nonnegative and bounded.

### **Equilibrium analysis**

**Lemma III.2.1.** *System (1) has nonnegative solutions and is bounded.*

*Proof:*

Let the initial conditions at  $t_0$  be  $S(t_0), I(t_0), A_u(t_0), A_v(t_0), R_u(t_0), R_v(t_0), D(t_0), V(t_0) \geq 0$ .

Note that  $\frac{dS}{dt} + \frac{dI}{dt} + \frac{dA_u}{dt} + \frac{dA_v}{dt} + \frac{dR_u}{dt} + \frac{dR_v}{dt} + \frac{dD}{dt} + \frac{dV}{dt} = 0$ . This implies that the solution  $S + I + A_u + A_v + R_u + R_v + D + V = N$ , the constant population number which is scaled to

1. From system (1), we assume for any  $t \geq 0$ :

$$\begin{aligned}
\frac{dS}{dt} &\geq -(\alpha_I I + \alpha_A A_u + \alpha_A A_v + \nu)S \\
\frac{dI}{dt} &\geq (\xi S \alpha_I - (\rho_s + \mu))I \\
\frac{dA_u}{dt} &\geq ((1 - \xi)S \alpha_A - \rho_{au})A_u \\
\frac{dA_v}{dt} &\geq ((1 - \tau)V \alpha_A - \rho_{av})A_v \\
\frac{dR_u}{dt} &\geq 0 \\
\frac{dR_v}{dt} &\geq 0 \\
\frac{dD}{dt} &\geq 0 \\
\frac{dV}{dt} &\geq -(1 - \tau)(\alpha_I I + \alpha_A A_u + \alpha_A A_v)V
\end{aligned} \tag{2}$$

Then the solutions at the initial conditions for each equation can be found with the separation of variables and integration:

$$\begin{aligned}
\int dS &\geq \int -(\alpha_I I + \alpha_A A_u + \alpha_A A_v + \nu)S dt \Rightarrow S(t) \geq S(t_0)e^{-(\alpha_I I + \alpha_A A_u + \alpha_A A_v + \nu)t_0} \geq 0 \\
\int dI &\geq \int (\xi S \alpha_I - (\rho_s + \mu))I dt \Rightarrow I(t) \geq I(t_0)e^{(\xi S \alpha_I - (\rho_s + \mu))t_0} \geq 0 \\
\int dA_u &\geq \int ((1 - \xi)S \alpha_A - \rho_{au})A_u dt \Rightarrow A_u(t) \geq A_u(t_0)e^{((1 - \xi)S \alpha_A - \rho_{au})t_0} \geq 0 \\
\int dA_v &\geq \int ((1 - \tau)V \alpha_A - \rho_{av})A_v dt \Rightarrow A_v(t) \geq A_v(t_0)e^{((1 - \tau)V \alpha_A - \rho_{av})t_0} \geq 0 \\
\int dR_u &\geq \int 0 dt \Rightarrow R_u(t) \geq R_u(t_0)e^{0t_0} \geq 0 \\
\int dR_v &\geq \int 0 dt \Rightarrow R_v(t) \geq R_v(t_0)e^{0t_0} \geq 0 \\
\int dD &\geq \int 0 dt \Rightarrow D(t) \geq D(t_0)e^{0t_0} \geq 0 \\
\int dV &\geq \int -(1 - \tau)(\alpha_I I + \alpha_A A_u + \alpha_A A_v)V dt \\
&\Rightarrow V(t) \geq V(t_0)e^{-(1 - \tau)(\alpha_I I + \alpha_A A_u + \alpha_A A_v)t_0} \geq 0
\end{aligned} \tag{3}$$

Therefore, the system has nonnegative solutions for  $t \geq t_0$ . As a consequence of being nonnegative and  $S + I + A_u + A_v + R_u + R_v + D + V = N = 1$ ,

$S(t) \leq N, I(t) \leq N, A_u(t) \leq N, A_v(t) \leq N, R_u(t) \leq N, R_v(t) \leq N, D(t) \leq N, V(t) \leq N$  and  $S(t) + I(t) + A_u(t) + A_v(t) + R_u(t) + R_v(t) + D(t) + V(t) = N$  for all  $t \geq t_0$ , and thus the system (1) is bounded.  $\square$

We observed the disease-free equilibrium when  $I = I^0 = 0, A_u = A_u^0 = 0, A_v = A_v^0 = 0$ : Then  $(S^0, I^0, A_u^0, A_v^0, R_u^0, R_v^0, D^0, V^0) = (S^0, 0, 0, 0, 0, 0, 0, V^0)$  since  $S^0 + V^0 = 1 = N$ .

Note that two cases were considered:

(i) If the daily vaccination rate  $v = 0$  then  $S^0$  and  $V^0$  are some constant portion of the population since, without daily vaccinations, there is no travel between susceptible and vaccinated compartments. In addition, no vaccine control measure existed when the first infected case occurs in Mississippi; therefore, there are no vaccinated individuals and  $V^0 = 0$ .

(ii) If the daily vaccination rate  $v \neq 0$  then all susceptible individuals eventually travel to  $V^0$  at the disease-free equilibrium, and eventually there are no susceptible individuals, making  $S^0 = 0$ .

The daily vaccination rate  $v$  can then be observed for the population of Mississippi within different scenarios. Since the first vaccine administration was on December 14, 2020, we assumed that some portion of the susceptible population is vaccinated by the time the Delta variant became the major variant in Mississippi on June 16, 2021 [21]. At this equilibrium point, we assumed that while the entire population was susceptible, some of the population may have received a vaccine. Since at this disease-free equilibrium point  $N(t_0) = S^0 + V^0$ , then  $S^0 = N(t_0) - V^0$  where  $N(t_0)$  is the initial population size, providing an equilibrium point of:

$$(N(t_0) - V^0, 0, 0, 0, 0, 0, 0, V^0) = (S^0, 0, 0, 0, 0, 0, 0, V^0).$$

This system represents an epidemic model which was used to observe the rapid outbreak of COVID-19 in Mississippi and does not observe population dynamics such as natural births and deaths in the population. Then the system does not have any

endemic-equilibrium points since the population is at a constant state and we cannot observe the disease with constant prevalence [5]. System (1) has an infinite number of disease-free equilibrium points since all populations stay within the system and the population stays constant, where at the disease-free equilibrium point, S and V can be any portion of the population. Therefore, we chose  $(S^0, 0, 0, 0, 0, 0, 0, V^0)$  as our disease-free equilibrium point.

## Reproduction Number

The reproduction number of the system is defined as the number of cases expected to stem from one infected case in a susceptible population. The reproduction number for the system was found using the next-generation matrix method by finding the spectral radius of the Jacobian matrix for the infected compartments  $I', A'_u, A'_v$  at the disease-free equilibrium [6]. Entries of matrix F represent new infections from those infected individuals. Entries of matrix G represent the outflow of infected compartments into other compartments such as recovered or deceased. Then,

$$F = \begin{bmatrix} \xi \alpha_I SI + \xi S \alpha_A A_u + \xi S \alpha_A A_v \\ (1 - \xi) S \alpha_I I + (1 - \xi) S \alpha_A A_u + (1 - \xi) S \alpha_A A_v \\ (1 - \tau) V \alpha_I I + (1 - \tau) V \alpha_A A_u + (1 - \tau) V \alpha_A A_v \end{bmatrix}$$

$$G = \begin{bmatrix} I(\rho_s + \mu) \\ \rho_{au} A_u \\ \rho_{av} A_v \end{bmatrix}$$

Then the Jacobian matrices for F and G are as follows:

$$F' = \begin{bmatrix} \xi S^0 \alpha_I & \xi S^0 \alpha_A & \xi S^0 \alpha_A \\ (1 - \xi) S^0 \alpha_I & (1 - \xi) S^0 \alpha_A & (1 - \xi) S^0 \alpha_A \\ (1 - \tau) V^0 \alpha_I & (1 - \tau) V^0 \alpha_A & (1 - \tau) V^0 \alpha_A \end{bmatrix}$$

$$G' = \begin{bmatrix} (\rho_s + \mu) & 0 & 0 \\ 0 & \rho_{au} & 0 \\ 0 & 0 & \rho_{av} \end{bmatrix}$$

The inverse of the matrix  $G'$ :

$$(G')^{-1} = \begin{bmatrix} \frac{1}{(\rho_s + \mu)} & 0 & 0 \\ 0 & \frac{1}{\rho_{au}} & 0 \\ 0 & 0 & \frac{1}{\rho_{av}} \end{bmatrix}$$

The next-generation matrix for system (1) at the disease-free equilibrium:

$$F'(G')^{-1} = \begin{bmatrix} \frac{\xi S^0 \alpha_I}{(\rho_s + \mu)} & \frac{\xi S^0 \alpha_A}{\rho_{au}} & \frac{\xi S^0 \alpha_A}{\rho_{av}} \\ \frac{(1-\xi)S^0 \alpha_I}{(\rho_s + \mu)} & \frac{(1-\xi)S^0 \alpha_A}{\rho_{au}} & \frac{(1-\xi)S^0 \alpha_A}{\rho_{av}} \\ \frac{(1-\tau)V^0 \alpha_I}{(\rho_s + \mu)} & \frac{(1-\tau)V^0 \alpha_A}{\rho_{au}} & \frac{(1-\tau)V^0 \alpha_A}{\rho_{av}} \end{bmatrix}$$

The reproduction number was found from the largest eigenvalue of  $F'(G')^{-1}$ .

$$\begin{aligned} \det(F'(G')^{-1} - \lambda I) &= \det \begin{bmatrix} \frac{\xi S^0 \alpha_I}{(\rho_s + \mu)} - \lambda & \frac{\xi S^0 \alpha_A}{\rho_{au}} & \frac{\xi S^0 \alpha_A}{\rho_{av}} \\ \frac{(1-\xi)S^0 \alpha_I}{(\rho_s + \mu)} & \frac{(1-\xi)S^0 \alpha_A}{\rho_{au}} - \lambda & \frac{(1-\xi)S^0 \alpha_A}{\rho_{av}} \\ \frac{(1-\tau)V^0 \alpha_I}{(\rho_s + \mu)} & \frac{(1-\tau)V^0 \alpha_A}{\rho_{au}} & \frac{(1-\tau)V^0 \alpha_A}{\rho_{av}} - \lambda \end{bmatrix} \\ &= \left( \frac{\xi S^0 \alpha_I}{(\rho_s + \mu)} - \lambda \right) \left| \begin{array}{cc} \frac{(1-\xi)S^0 \alpha_A}{\rho_{au}} - \lambda & \frac{(1-\xi)S^0 \alpha_A}{\rho_{av}} \\ \frac{(1-\tau)V^0 \alpha_A}{\rho_{au}} & \frac{(1-\tau)V^0 \alpha_A}{\rho_{av}} - \lambda \end{array} \right| - \left( \frac{\xi S^0 \alpha_A}{\rho_{au}} \right) \left| \begin{array}{cc} \frac{(1-\xi)S^0 \alpha_I}{(\rho_s + \mu)} & \frac{(1-\xi)S^0 \alpha_A}{\rho_{av}} \\ \frac{(1-\tau)V^0 \alpha_I}{(\rho_s + \mu)} & \frac{(1-\tau)V^0 \alpha_A}{\rho_{av}} - \lambda \end{array} \right| \\ &\quad + \left( \frac{\xi S^0 \alpha_A}{\rho_{av}} \right) \left| \begin{array}{cc} \frac{(1-\xi)S^0 \alpha_I}{(\rho_s + \mu)} & \frac{(1-\xi)S^0 \alpha_A}{\rho_{au}} - \lambda \\ \frac{(1-\tau)V^0 \alpha_I}{(\rho_s + \mu)} & \frac{(1-\tau)V^0 \alpha_A}{\rho_{au}} \end{array} \right| \\ &= \left( \frac{\xi S^0 \alpha_I}{(\rho_s + \mu)} - \lambda \right) \left[ \frac{(1-\xi)S^0 \alpha_A (1-\tau)V^0 \alpha_A}{\rho_{au} \rho_{av}} \right. \\ &\quad \left. - \lambda \left( \frac{(1-\xi)S^0 \alpha_A}{\rho_{au}} + \frac{(1-\tau)V^0 \alpha_A}{\rho_{av}} \right) + \lambda^2 - \frac{(1-\xi)S^0 \alpha_A (1-\tau)V^0 \alpha_A}{\rho_{av} \rho_{au}} \right] \\ &\quad - \left( \frac{\xi S^0 \alpha_A}{\rho_{au}} \right) \left[ \frac{(1-\xi)S^0 \alpha_I (1-\tau)V^0 \alpha_A}{(\rho_s + \mu) \rho_{av}} - \lambda \frac{(1-\xi)S^0 \alpha_I}{\rho_s + \mu} - \frac{(1-\xi)S^0 \alpha_A (1-\tau)V^0 \alpha_I}{\rho_{av} (\rho_s + \mu)} \right] \\ &\quad + \left( \frac{\xi S^0 \alpha_A}{\rho_{av}} \right) \left[ \frac{(1-\xi)S^0 \alpha_I (1-\tau)V^0 \alpha_A}{(\rho_s + \mu) \rho_{au}} - \frac{(1-\xi)S^0 \alpha_A (1-\tau)V^0 \alpha_I}{(\rho_s + \mu) \rho_{au}} + \lambda \frac{(1-\tau)V^0 \alpha_I}{\rho_s + \mu} \right] \\ &= -\lambda^2 \left( \frac{(1-\xi)S^0 \alpha_A}{\rho_{au}} + \frac{(1-\tau)V^0 \alpha_A}{\rho_{av}} + \frac{\xi S^0 \alpha_I}{(\rho_s + \mu)} - \lambda \right) \end{aligned}$$

Then the reproduction number of the system is

$$\mathcal{R}_0 = \frac{(1-\xi)S^0 \alpha_A}{\rho_{au}} + \frac{(1-\tau)V^0 \alpha_A}{\rho_{av}} + \frac{\xi S^0 \alpha_I}{(\rho_s + \mu)} \quad (4)$$

which is the sum of the secondary infections caused by those asymptomatic susceptible, vaccinated, and symptomatic susceptible.

*Remark III.3.1.* If  $v \neq 0$  then  $S^0$  eventually becomes 0 and the basic reproduction number becomes the effective reproduction number

$$\mathcal{R}_e = \frac{(1-\tau)V^0\alpha_A}{\rho_{av}}$$

since the susceptible population is now vaccinated and therefore immune except for breakthrough cases. Thus  $\mathcal{R}_e$  will depend on vaccine effectiveness  $\tau$ . This assumption depicts how effective the vaccine must be to produce the smallest effective reproduction number feasible for COVID-19 in Mississippi.

### Linear Stability Analysis

**Theorem III.4.1.** *Let  $(S^0, 0, 0, 0, 0, 0, 0, V^0)$  be a disease-free equilibrium. Then the ASIRD – V system is locally asymptotically stable if the basic reproduction number  $\mathcal{R}_0 < 1$ . Conversely, the system is locally unstable if the basic reproduction number  $\mathcal{R}_0 > 1$ .*

*Proof:*

At the disease-free equilibrium, we determined the Jacobian matrix of the ASIRD – V system:

$$J_0 = \begin{bmatrix} 0 & -S^0\alpha_I & -S^0\alpha_A & -S^0\alpha_A & 0 & 0 & 0 & 0 \\ 0 & \xi\alpha_I S^0 - (\rho_s + \mu) & \xi\alpha_A S^0 & \xi\alpha_A S^0 & 0 & 0 & 0 & 0 \\ 0 & (1-\xi)\alpha_I S^0 & (1-\xi)\alpha_A S^0 - \rho_{au} & (1-\xi)\alpha_A S^0 & 0 & 0 & 0 & 0 \\ 0 & \alpha_I(1-\tau)V^0 & \alpha_A(1-\tau)V^0 & \alpha_A(1-\tau)V^0 - \rho_{av} & 0 & 0 & 0 & 0 \\ 0 & \rho_s & \rho_{au} & 0 & 0 & 0 & 0 & 0 \\ 0 & 0 & 0 & \rho_{av} & 0 & 0 & 0 & 0 \\ 0 & \mu & 0 & 0 & 0 & 0 & 0 & 0 \\ 0 & S^0 & \alpha_I(1-\tau)V^0 & \alpha_A(1-\tau)V^0 & \alpha_A(1-\tau)V^0 & 0 & 0 & 0 \end{bmatrix}$$

$$(J_0 - \lambda I) = \begin{bmatrix} -\lambda & -S^0\alpha_I & -S^0\alpha_A & -S^0\alpha_A & 0 & 0 & 0 & 0 \\ 0 & \xi\alpha_I S^0 - (\rho_s + \mu) - \lambda & \xi\alpha_A S^0 & \xi\alpha_A S^0 & 0 & 0 & 0 & 0 \\ 0 & (1-\xi)\alpha_I S^0 & (1-\xi)\alpha_A S^0 - \rho_{au} - \lambda & (1-\xi)\alpha_A S^0 & 0 & 0 & 0 & 0 \\ 0 & \alpha_I(1-\tau)V^0 & \alpha_A(1-\tau)V^0 & \alpha_A(1-\tau)V^0 - \rho_{av} - \lambda & 0 & 0 & 0 & 0 \\ 0 & \rho_s & \rho_{au} & 0 & -\lambda & 0 & 0 & 0 \\ 0 & 0 & 0 & \rho_{av} & 0 & -\lambda & 0 & 0 \\ 0 & \mu & 0 & 0 & 0 & 0 & -\lambda & 0 \\ 0 & \alpha_I(1-\tau)V^0 & \alpha_A(1-\tau)V^0 & \alpha_A(1-\tau)V^0 & 0 & 0 & 0 & -\lambda \end{bmatrix}$$



Calculating the characteristic polynomial of the Jacobian matrix presented the equation

$$\begin{aligned} \det(J_0 - \lambda I) = & -\lambda[(\xi \alpha_I S^0 - (\rho_s + \mu) - \lambda)[((1 - \xi)\alpha_A S^0 - \rho_{au} - \lambda)(\alpha_A(1 - \tau)V^0 - \rho_{av} - \lambda)\lambda^4 \\ & - (1 - \xi)\alpha_A S^0(\alpha_A(1 - \tau)V^0)\lambda^4] \\ & - \xi \alpha_A S^0[(1 - \xi)\alpha_I S^0(\alpha_A(1 - \tau)V^0 - \rho_{av} - \lambda)\lambda^4 - (1 - \xi)\alpha_A S^0(\alpha_I(1 - \tau)V^0)\lambda^4] \\ & + \xi \alpha_A S^0[(1 - \xi)\alpha_I S^0(\alpha_A(1 - \tau)V^0)\lambda^4 - ((1 - \xi)\alpha_A S^0 - \rho_{au} - \lambda)(\alpha_I(1 - \tau)V^0)\lambda^4] \end{aligned}$$

which is equivalent to

$$\begin{aligned} & -\lambda^5[(\xi \alpha_I S^0 - (\rho_s + \mu) - \lambda)[\lambda^2 + \lambda(\rho_{au} + \rho_{av} - (1 - \xi)\alpha_A S^0 - \alpha_A(1 - \tau)V^0) \\ & - (1 - \xi)\alpha_A S^0 \rho_{av} - \rho_{au}\alpha_A(1 - \tau)V^0 + \rho_{au}\rho_{av}] \\ & + \xi \alpha_A S^0[(1 - \xi)\alpha_I S^0(\rho_{av} + \lambda) + (\alpha_I(1 - \tau)V^0)(\rho_{au} + \lambda)]. \end{aligned}$$

Reducing and substituting the reproduction number provided the following eighth order characteristic polynomial:

$$\begin{aligned} & \lambda^5[\lambda^3 - \lambda^2(\xi \alpha_I S^0 - (\rho_s + \mu) - \rho_{au} - \rho_{av} + (1 - \xi)\alpha_A S^0 + \alpha_A(1 - \tau)V^0) \\ & - \lambda(\xi \alpha_I S^0(\rho_{av} + \rho_{au}) - (\rho_s + \mu)(\rho_{av} + \rho_{au} - (1 - \xi)\alpha_A S^0 - \alpha_A(1 - \tau)V^0) \\ & + (1 - \xi)\alpha_A S^0 \rho_{av} + \alpha_A(1 - \tau)V^0 \rho_{au} - \rho_{au}\rho_{av}) \\ & + (\rho_s + \mu)\rho_{au}\rho_{av}(1 - \mathcal{R}_0)]. \end{aligned}$$

We used the Routh-Hurwitz stability criterion on the third order polynomial

$$\begin{aligned} & \lambda^3 - \lambda^2(\xi \alpha_I S^0 - (\rho_s + \mu) - \rho_{au} - \rho_{av} + (1 - \xi)\alpha_A S^0 + \alpha_A(1 - \tau)V^0) \\ & - \lambda(\xi \alpha_I S^0(\rho_{av} + \rho_{au}) - (\rho_s + \mu)(\rho_{av} + \rho_{au} - (1 - \xi)\alpha_A S^0 - \alpha_A(1 - \tau)V^0) \\ & + (1 - \xi)\alpha_A S^0 \rho_{av} + \alpha_A(1 - \tau)V^0 \rho_{au} - \rho_{au}\rho_{av}) \\ & + (\rho_s + \mu)\rho_{au}\rho_{av}(1 - \mathcal{R}_0) \end{aligned}$$

which can be shaped as

$$\lambda^3 - a_2 \lambda^2 - a_1 \lambda + a_0$$

where

$$a_2 = -(\xi \alpha_I S^0 - (\rho_s + \mu) - \rho_{au} - \rho_{av} + (1 - \xi) \alpha_A S^0 + \alpha_A (1 - \tau) V^0)$$

$$a_1 = -(\xi \alpha_I S^0 (\rho_{av} + \rho_{au}) - (\rho_s + \mu) (\rho_{av} + \rho_{au} - (1 - \xi) \alpha_A S^0 - \alpha_A (1 - \tau) V^0) \\ + (1 - \xi) \alpha_A S^0 \rho_{av} + \alpha_A (1 - \tau) V^0 \rho_{au} - \rho_{au} \rho_{av})$$

$$a_0 = (\rho_s + \mu) \rho_{au} \rho_{av} (1 - \mathcal{R}_0)$$

to determine that the polynomial is stable and the system has control of the disease if and only if (i) coefficients  $a_2$  and  $a_0$  are positive and (ii)  $a_2 a_1 > a_0$  [14]. Note that

$$\xi, \alpha_I, \alpha_A, \rho_s, \mu, \rho_{av}, \rho_{au}, \tau, (1 - \xi), (1 - \tau), S^0, V^0 > 0.$$

(i) Let  $\mathcal{R}_0$  be defined as equation (4) and  $\mathcal{R}_0 < 1$ . Then  $1 - \mathcal{R}_0 > 0$ . Since

$(\rho_s + \mu) \rho_{au} \rho_{av} > 0$  and  $(1 - \mathcal{R}_0) > 0$ , then  $a_0 = (\rho_s + \mu) \rho_{au} \rho_{av} (1 - \mathcal{R}_0) > 0$ . Similarly, if  $\mathcal{R}_0 < 1$  then  $0 < \frac{(1 - \xi) S^0 \alpha_A}{\rho_{au}} < 1$ ,  $0 < \frac{(1 - \tau) V^0 \alpha_A}{\rho_{av}} < 1$ , and  $0 < \frac{\xi S^0 \alpha_I}{(\rho_s + \mu)} < 1$ . Rearranging,

$$a_2 = \rho_{au} \left[ 1 - \frac{(1 - \xi) S^0 \alpha_A}{\rho_{au}} \right] + \rho_{av} \left[ 1 - \frac{(1 - \tau) V^0 \alpha_A}{\rho_{av}} \right] + (\rho_s + \mu) \left[ 1 - \frac{\xi S^0 \alpha_I}{(\rho_s + \mu)} \right] \quad (5)$$

Then  $\left[ 1 - \frac{(1 - \xi) S^0 \alpha_A}{\rho_{au}} \right] > 0$ ,  $\left[ 1 - \frac{(1 - \tau) V^0 \alpha_A}{\rho_{av}} \right] > 0$ , and  $\left[ 1 - \frac{\xi S^0 \alpha_I}{(\rho_s + \mu)} \right] > 0$ . Since

$\rho_{au} > 0$ ,  $\rho_{av} > 0$  and  $(\rho_s + \mu) > 0$ , then  $a_2 > 0$ .

Therefore, if  $\mathcal{R}_0 < 1$ , then  $a_2 > 0$  and  $a_0 > 0$ .

(ii) Let  $\mathcal{R}_0$  be defined as equation (4) and  $\mathcal{R}_0 < 1$ . From (i), we have  $a_2 > 0$  and  $a_0 > 0$ . We

also have  $0 < \frac{(1 - \xi) S^0 \alpha_A}{\rho_{au}} < 1$ ,  $0 < \frac{(1 - \tau) V^0 \alpha_A}{\rho_{av}} < 1$ , and  $0 < \frac{\xi S^0 \alpha_I}{(\rho_s + \mu)} < 1$ . In addition,

$0 < \frac{(1 - \xi) S^0 \alpha_A}{\rho_{au}} + \frac{(1 - \tau) V^0 \alpha_A}{\rho_{av}} < 1$  Using equation (5),

$$a_2 a_1 - a_0 = \\ a_2 \left[ (\rho_s + \mu) \left[ (\rho_{au} + \rho_{av}) \left( 1 - \frac{\xi S^0 \alpha_I}{(\rho_s + \mu)} \right) - (1 - \xi) \alpha_A S^0 - (1 - \tau) \alpha_A S^0 \right] \right] \\ + \left[ a_2 - (\rho_s + \mu) \left[ 1 - \frac{\xi S^0 \alpha_I}{(\rho_s + \mu)} \right] \right] \left[ \rho_{au} \rho_{av} \left[ 1 - \left( \frac{(1 - \xi) S^0 \alpha_A}{\rho_{au}} + \frac{(1 - \tau) S^0 \alpha_A}{(\rho_{av})} \right) \right] \right] \\ + \frac{\xi S^0 \alpha_I}{(\rho_s + \mu)} \left( \frac{(1 - \xi) S^0 \alpha_A}{\rho_{au}} + \frac{(1 - \tau) V^0 \alpha_A}{\rho_{av}} \right)$$

Then  $a_2 a_1 - a_0 > 0$  if  $\mathcal{R}_0 < 1$ .

Then by (i) and (ii), the system is stable when  $R_0 < 1$  and unstable when  $R_0 > 1$ .  $\square$

Now, we proved that our model can simulate the spread of COVID-19 as well as the vaccine administration in Mississippi with realistic numbers. With nonnegative and bounded solutions, no compartment in our model can have negative population values. In addition, our model is endemic, meaning we defined  $(S^0, 0, 0, 0, 0, 0, 0, V^0)$  as our disease-free equilibrium since we were not observing a constant prevalence in short-time periods. The basic reproduction number  $\mathcal{R}_0$  of our system is derived from all infectious compartments, and we determined the stability of the system in relation to this number.

In the next chapter, we applied our *ASIRD* – *V* model to four different time periods of the COVID-19 pandemic in Mississippi. Two of these observations occurred before vaccine development while two explored observations during active vaccine administration in Mississippi. We used the mathematical programming language MATLAB to numerically solve our system with parameters optimized to death and vaccine data downloaded from the CDC. Since the vaccine efficacy  $\tau$  is given by the CDC, we optimized eight out of nine parameters using the sum of least squares method. By minimizing the difference between the solutions *D* and *V* against the death and vaccine data, the sum of least squares objective function computed the best parameter values to model the spread of COVID-19 and vaccine administration. We have a list of eight unknown nonnegative parameters

$p = (\alpha_I, \alpha_A, \rho_s, \rho_{au}, \rho_{av}, \nu, \mu, \xi)$  optimized for each time period  $t$  from  $k$  to  $K$  days where  $D_{MS}(t_k)$  is the cumulative total confirmed deaths data on the  $k^{th}$  day and  $V_{MS}(t_k)$  is the cumulative vaccine data on the  $k^{th}$  day. Both data sets were scaled to 1. Then the following function was minimized:

$$L(p) = \sqrt{\sum_{k=1}^K \left[ \left( \frac{D_{MS}(t_k)}{2.96 \times 10^6} - D(t_k; p) \right)^2 + \left( \frac{V_{MS}(t_k)}{2.96 \times 10^6} - V(t_k; p) \right)^2 \right]} \quad (6)$$

We wanted to observe how well our model could simulate and predict these time periods and understand how this disease spread among Mississippians.

## CHAPTER IV: RESULTS

In this study, we applied the  $ASIRD - V$  system to simulate the spread of COVID-19 in Mississippi for four time periods, separated into periods with and without vaccine administration. The first two time periods spanned 32 days from the first confirmed case of COVID-19 in Mississippi on March 4, 2020 to April 4, 2020. In these two time spans, we used only death data from the CDC in optimizing our parameters using the sum of least squares method [13]. For the first time span, the initial condition for infected  $I(0)$  used confirmed cases data on March 4. Since there was no data on the initial number of asymptomatic cases, or any data on asymptomatic cases, the initial condition for unvaccinated asymptomatic cases  $A_u(0)$  was estimated and not verifiable. The second time span is a continuation of the first time span, starting on March 23, 2020 where the parameters were observed to need re-optimization. Therefore, the initial conditions for March 23, 2020 to April 4, 2020 are the values given by the  $ASIRD - V$  model on March 23, 2020 using the parameters optimized in the first time span. The next two time periods used only the death data and the vaccine data given by the CDC to optimize parameters using the sum of least squares method [13] [12]. These two time spans were further within the timeline of the pandemic, and since the exact number of infected individuals on a particular day is difficult to obtain and verify, the initial number of infected individuals was included in the model as a parameter to be estimated, which can be used to check the validity of the model. However, the fourth time period clearly shows this decision must be revised for any future research.

### **Without Vaccine Administration**

The first 20 days of the pandemic in Mississippi were modeled with parameters optimized from March 4, 2020 to March 23, 2020. An additional three days were predicted using these optimized parameters to verify any changes that occur. The following initial conditions were used:

$$\begin{aligned}
I(0) &= \frac{4}{2960000} = 1.35 \times 10^{-6} & A_u(0) &= 1.24 \times 10^{-6} & A_v(0) &= 0 \\
R_u(0) &= 0 & R_v(0) &= 0 & D(0) &= 0 & V(0) &= 0 \\
S(0) &= 1 - (I(0) + A_u(0))
\end{aligned} \tag{7}$$

where  $I(0)$  is the initial number of confirmed cases on March 4, 2020, divided by the total population of Mississippi, and  $A_u(0)$  was found through trial and error for a realistic model with reasonable numbers, landing at about 3 unvaccinated asymptomatic individuals. Note that the initial condition for asymptomatic individuals is not verifiable since no data for asymptomatic cases were collected for Mississippi. The initial susceptible population  $S(0)$  is 1 minus the sum of the infected symptomatic and asymptomatic since the rest of the compartments do not yet contain any individuals. To observe the effect of the changes in health policies during the pandemic without a vaccine, the necessary parameters of the model were optimized with death data from March 4, 2020 to March 23, 2020 using the sum of least squares method. Since during this time there were no vaccines, optimization of the parameters  $\rho_{av} = 0$  and  $v = 0$  was not necessary. These parameter values made the model identical to the *ASIRD* model since  $V$ ,  $A_v$ , and  $R_v$  were valued at 0 for this time. The parameter values were used to predict the next 3 days when Mississippi Governor Tate Reeves passed the MS Executive Order 1463: Stay at Home from March 24, 2020 to April 17, 2020 [22]. The parameters were optimized to the following values:

$$\alpha_I = 0.00587 \quad \alpha_A = 1.62 \quad \xi = 0.773 \quad \rho_s = 0.00979 \quad \rho_{au} = 0.289 \quad \mu = 0.0981 \tag{8}$$

In the numerical solution of the system, we computed the reproduction number  $\mathcal{R}_0$  to be approximately 1.32. Since this value is greater than 1, we observed an epidemic of COVID-19 in Mississippi. The parameter values for these figures were also reasonable for the reality of the pandemic. The asymptomatic infection rate  $\alpha_A$  was greater than the symptomatic infection rate  $\alpha_I$  while the unvaccinated asymptomatic recovery rate  $\rho_{au}$  was greater than the symptomatic recovery rate  $\rho_s$ . Since there were so few symptomatic

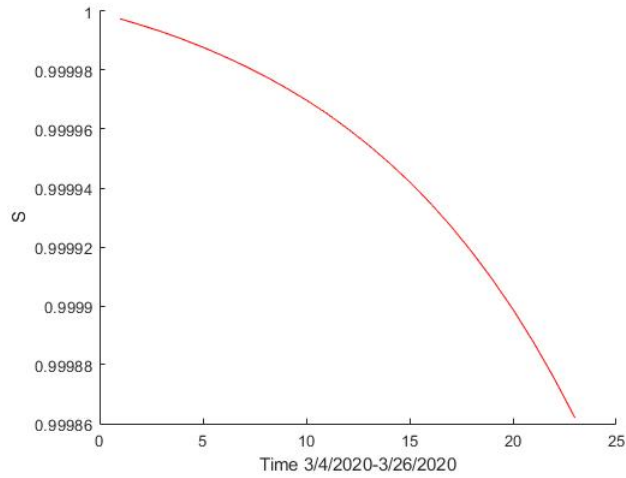


Figure 2: Solution of Susceptible Population from March 4 to March 26, 2020

Parameters are optimized to the following values:

$\alpha_I = 0.00587, \alpha_A = 1.62, \xi = 0.773, \rho_s = 0.00979, \rho_{au} = 0.289, \mu = 0.0981$ . Additionally,  
 $\rho_{av} = 0, \nu = 0, \tau = 0$  and  $\mathcal{R}_0 = 1.32$

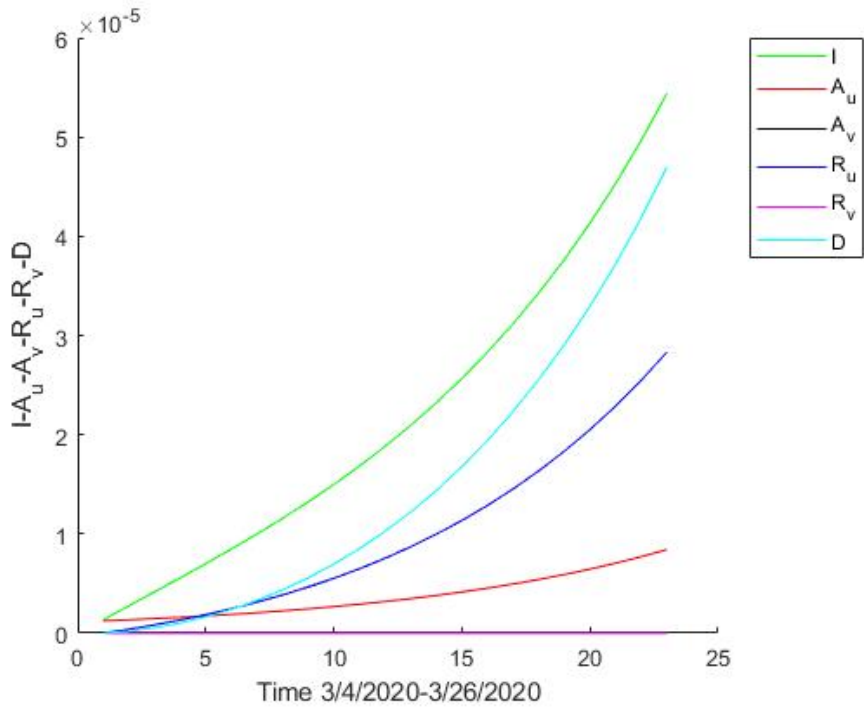


Figure 3:  $I, A_u, A_v, R_u, R_v, D$  from March 4 to March 26, 2020

Since there is no vaccine at this time,  $A_v = R_v = 0$  for all 23 days

infected, it is reasonable to see that the rate of infection for symptomatic individuals was small. In addition, it was reasonable to assume that at the beginning of the pandemic, there

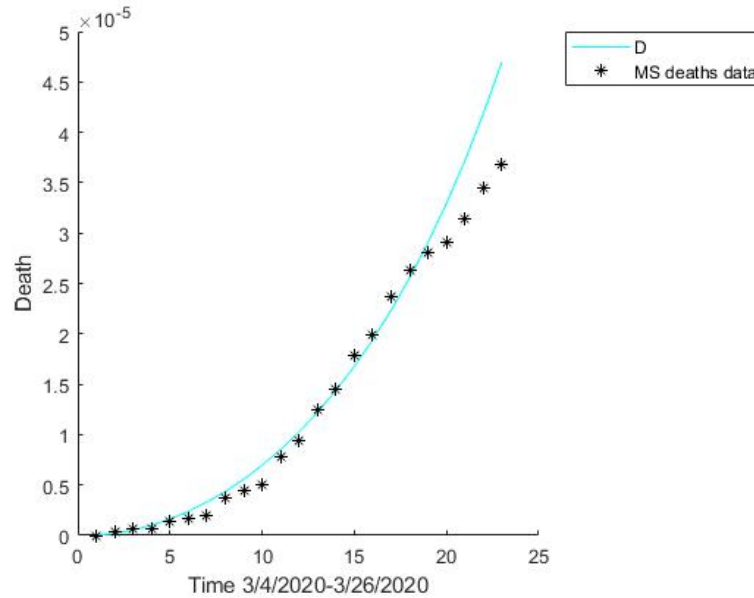


Figure 4: Data fitting for  $D$  from March 4 to March 23, 2020

This graph is using the first 20 days of death data by the Centers for Disease Control [13] and predicts March 24 to March 26, 2020 with optimized parameters.

were individuals who had COVID-19 who showed few symptoms or simply were not tested for this disease because of the lack of testing and knowledge. Thus these individuals spread the disease faster since they were not quarantined or did not observe the necessary health protocols for infected individuals. However, since the number of asymptomatic individuals is unknown and cannot be verified by data, these values for asymptomatic individuals should not be considered accurate. The recovery rates reflect how treatment for symptomatically infected individuals was new and lacked the resources and knowledge of the symptoms of COVID-19 while individuals with little to no symptoms recovered faster than those with severe symptoms. Figures 2 and 3 show the COVID-19 epidemic with the reproduction number  $\mathcal{R}_0 = 1.32$ . In figure 2, as more people became infected, the susceptible population decreased. In figure 3, as the disease spread among the susceptible population, more people became infected and either recovered or died. Finally, Figure 4 shows the impact of restricting group sizes in the population as well as social-distancing measures and wearing masks as a preventative against the spread of COVID-19. Near the day of the Executive Stay at Home Order, the system no longer reflected the deceased

number of individuals as verifiable by the CDC death data. This change indicates some effect of the Stay at Home Order, and the optimized parameters no longer represent the spread of COVID-19 in Mississippi. Thus, the next time period of the pandemic required the parameters to be re-optimized to account for the reaction of the population.

Beginning on the day of the Stay at Home Executive Order, the time period March 23, 2020 to April 4, 2020 was modeled with parameters optimized for the period March 23 to April 1, 2020. On April 1, 2020, Mississippi Governor Tate Reeves passed Executive Order 1466 which closed all nonessential businesses [22]. The next day, the CDC officially recommended the use of masks and social distancing to prevent the spread of COVID-19. Since this time represents nearly the beginning of the pandemic, initial conditions for the vaccinated and its subsequent infected and recovered populations were assumed to be 0. The following are the initial conditions computed by the previous model with parameters values of (8) on March 23:

$$\begin{aligned}
 I(0) &= 4.132 \times 10^{-5} & A_u(0) &= 6.4555 \times 10^{-6} & A_v(0) &= 0 \\
 R_u(0) &= 2.051 \times 10^{-5} & R_v(0) &= 0 & D(0) &= 2.905 \times 10^{-5} & V(0) &= 0 \\
 S(0) &= 1 - (I(0) + A_u(0) + R_u(0) + D(0))
 \end{aligned} \tag{9}$$

The initial numbers of symptomatic  $I(0)$ , unvaccinated asymptomatic  $A_u(0)$ , and unvaccinated recovered  $R_u(0)$  were determined by their values on March 23 as observed with the previously optimized parameters (8), approximately 122, 19, and 70 individuals respectively. The initial number of deaths  $D(0)$  was determined by the cumulative death data given by the CDC for March 23. Again, since there was no vaccine during this time,  $A_v(0) = R_v(0) = V(0) = 0$ , and we optimized the system identical to the *ASIRD* model. The parameters were optimized to the following values:

$$\begin{aligned}
 \alpha_I &= 0.9646 & \alpha_A &= 0.3328 & \xi &= 0.1538 \\
 \rho_s &= 0.2889 & \rho_{au} &= 0.1225 & \mu &= 0.07644
 \end{aligned} \tag{10}$$

Figures 5, 6, and 7 depict the effects of the population following these changes in health policies. Firstly, the basic reproduction number  $\mathcal{R}_0 = 2.705$  signified that people



were infecting more people than before, showing the infectiousness of this disease and continuing the epidemic. The parameter values optimized to the death data were also shown to be reasonable for this time in the pandemic. The symptomatic infection rate  $\alpha_I$  was now greater than the asymptomatic infection rate  $\alpha_A$  while the symptomatic recovery rate  $\rho_s$  grew to be greater than the asymptomatic recovery rate  $\rho_{au}$ . Figure 5 shows the susceptible population decreased as individuals became either symptomatic or asymptomatic, and Figure 6 shows the spread of COVID-19 as more people became aware of its persistence, with the last three days predicted. As more people become symptomatically infected, the larger the rate of symptomatic infection becomes. Similarly, an asymptomatic individual either does not realize they have the disease or shows such few symptoms as not to isolate themselves and thus infect a significant amount of the population. By this time, the number of deaths was low, reflecting the time before the overcrowding of hospitals and the lack of ventilators.

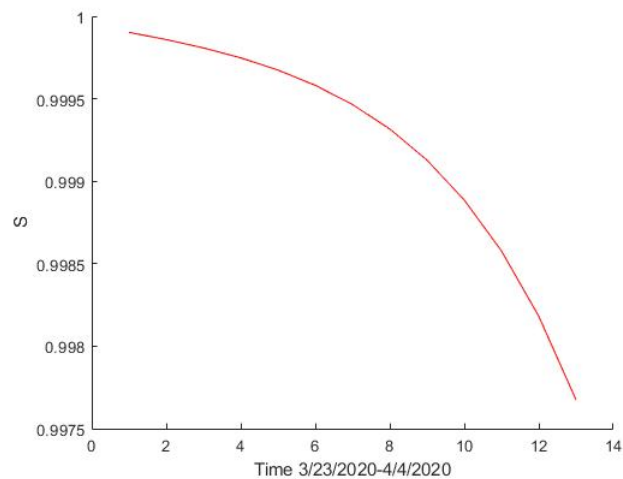


*Figure 5: S from March 23 to April 4, 2020*

Figure 7 depicts the changes when individuals began applying health protocols and following strict guidelines recommended by the Centers for Disease Control in Mississippi. The data fit well for this time period; however, when the parameters (10) were used to predict the next few days, the system was no longer accurate when verified with the death data. The difference between the model and the data shows the lives that were saved while

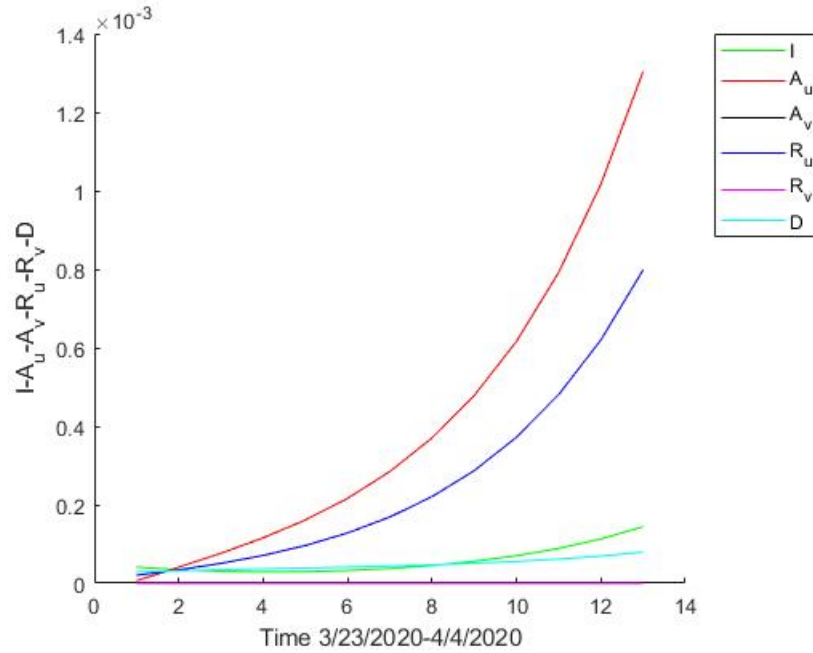


Figure 6:  $I, A_u, A_v, R_u, R_v, D$  from March 23 to April 4, 2020  
 Here,  $\alpha_I = 0.9646, \alpha_A = 0.3328, \xi = 0.1538, \rho_s = 0.2889, \rho_{au} = 0.1225, \mu = 0.07644$   
 Additionally,  $\mathcal{R}_0 = 2.705$ . Since there is no vaccine at this time,  $A_v = R_v = 0$ .

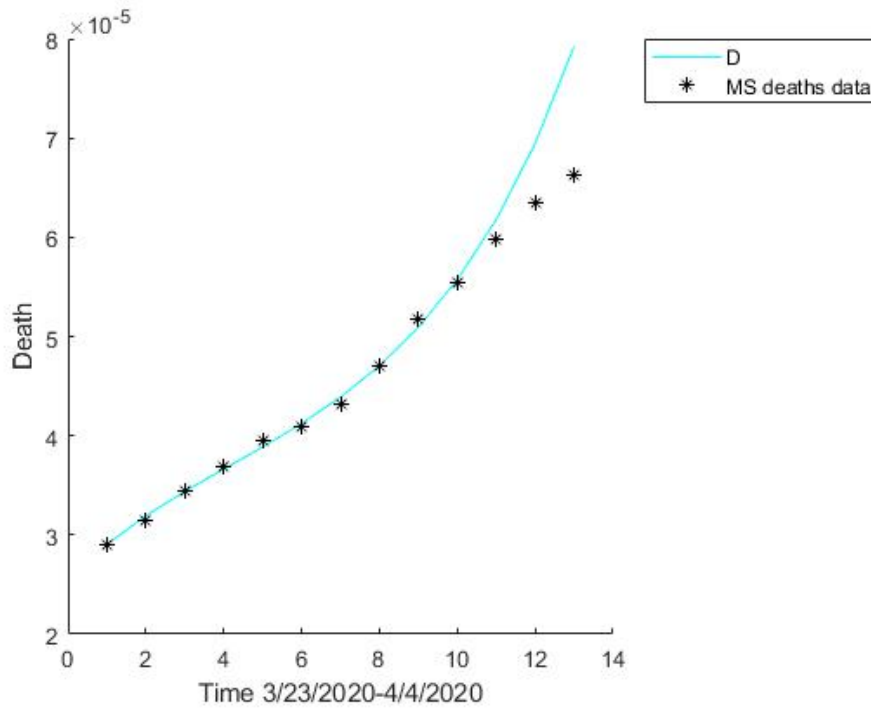


Figure 7: Data fitting for  $D$ , from March 23 to April 1, 2020

the executive order shut down bars, restaurants, and schools, as well as wearing a mask as recommended by the CDC. After April 1, the system was no longer a good model with the current optimized parameters (10). Due to the reactions to policies and more proactive health guidelines, the parameters required re-optimization for any subsequent time periods.

### **With Vaccine Administration**

The first dose of the vaccine available in Mississippi was the Pfizer vaccine on December 16, 2020. By this time, only those 65 years and older and those with underlying health problems were eligible to receive the vaccine. Additionally, two doses of the Pfizer or Moderna mRNA vaccines are required to become fully vaccinated; the second dose of Moderna is given 28 days after the first and the second dose of Pfizer is given 21 days after the first. Between the first and second doses, both mRNA vaccines have effectiveness between 40 and 80 percent at preventing the contraction of COVID-19 [18]. The Janssen vaccine only requires one dose, and studies have shown its effectiveness at prevention to be approximately 69% [20].

The ASIRD-V model was used to observe the effects of disease prevention with a vaccine. To observe the effect of distributing vaccines to Mississippians, the first week of vaccine administration was modeled with optimized parameters; these parameters were then used to predict the next five days in comparison to the data provided by the CDC. The only two initial conditions that are verifiable and accurate are the initial deceased  $D(0)$  and the initial vaccinated with one dose  $V(0)$ . There was no data available to tell us exactly how many people were currently infected with COVID-19 in Mississippi; although the value can be estimated with confirmed cases data, the exact initial number of infected  $I(0)$  on a particular day cannot be determined accurately by confirmed cases. Instead, we approximated  $I(0)$  with the number of confirmed cases, although not exactly the number of cumulative confirmed cases from the past two weeks. Since we modeled the pandemic without modeling all previous time periods, the initial conditions were approximated to the best possible values to obtain reasonable parameters. Therefore, the solutions to the system

for this time period do not represent an accurate depiction of the spread of COVID-19 in Mississippi. To optimize the parameters from December 16, 2020 to December 22, 2020, the following initial conditions were used:

$$\begin{aligned}
I(0) &= 0.0075433 & A_u(0) &= 0.0075909 & A_v(0) &= 3.38 \times 10^{-7} & R_u(0) &= 0.075115 \\
R_v(0) &= 0 & D(0) &= 0.0016928 & V(0) &= 1.6885 \times 10^{-6} \\
S(0) &= 1 - (I(0) + A_u(0) + A_v(0) + R_u(0) + R_v(0) + D(0) + V(0))
\end{aligned} \tag{11}$$

The initial number of symptomatic infected  $I(0)$  was determined by an estimated number of cases in Mississippi according to CDC new cases data for December 16, approximately 22,330 infected individuals. The initial number of unvaccinated asymptomatic  $A_u(0)$  was determined through trial and error in finding a realistic model with reasonable parameters and accounts for approximately 22,470 individuals. The initial condition for  $A_v(0)$  was assumed and represents one person who became infected after receiving only one dose of the vaccine. Since the initial condition started on the first day of vaccine administration, we assumed there were no initial individuals vaccinated and recovered from the disease. By using the CDC data on vaccinations, we assumed the first week of vaccinations composed of only first dose mRNA vaccines, with initially only 5 individuals vaccinated [12]. Additionally, since the Janssen vaccine was not administered during the first week, the vaccine effectiveness ( $\tau$ ) of only one dose for both mRNA vaccines was assumed to be 89%.

Lastly, we again used the CDC deaths data on December 16 to determine the initial number of deceased individuals. By using both vaccine data and death data from the CDC, the parameters were optimized to the following values:

$$\begin{aligned}
\alpha_I &= 0.05093 & \alpha_A &= 0.001625 & \xi &= 0.05124 & \rho_s &= 0 \\
\rho_{au} &= 0.04999 & \rho_{av} &= 1.75038 \times 10^{-10} & \mu &= 0.001695 & \nu &= 0.0002026
\end{aligned} \tag{12}$$

Figures 8 through 14 depict the compartments of the system as COVID-19 spread rapidly with a calculated reproduction number  $\mathcal{R}_0 = 3.15$  and a prediction of the last five days.

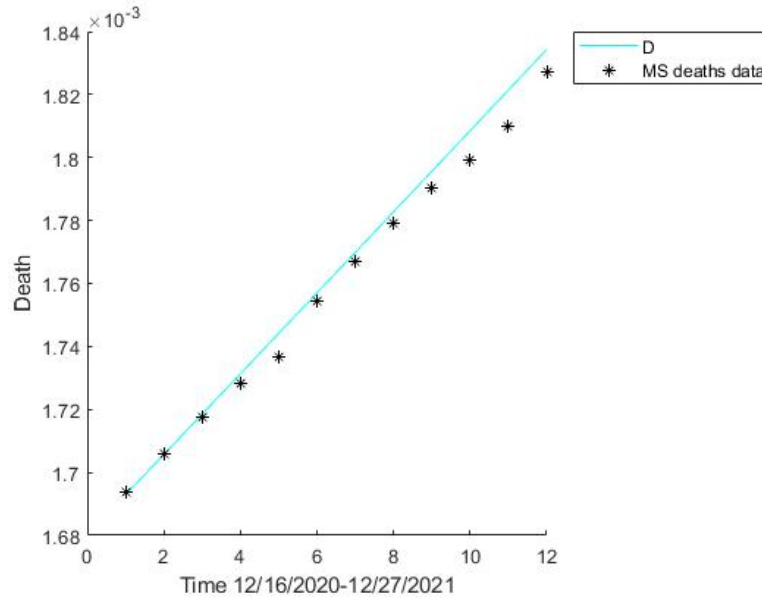


Figure 8: Data fitting for  $D$ , from December 16 to December 22, 2020

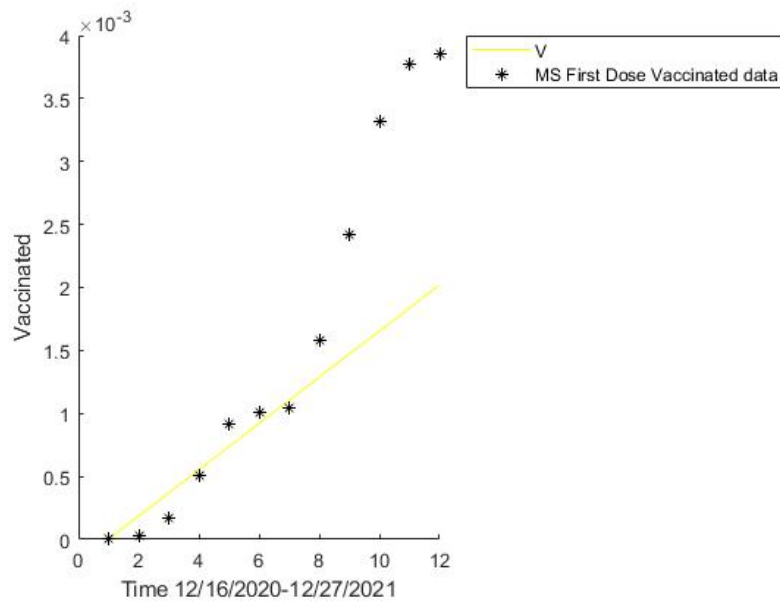


Figure 9: Data fitting for  $V$  from December 16 to December 22, 2020

From Figures 8 and 9, the first dose of vaccine administration has little to no effect on the number of rising deaths caused by COVID-19 during this time. Figure 10 shows that as the vaccine administration began and the epidemic continued, very few people within the susceptible population moved to the vaccinated population. The vaccine data shows the

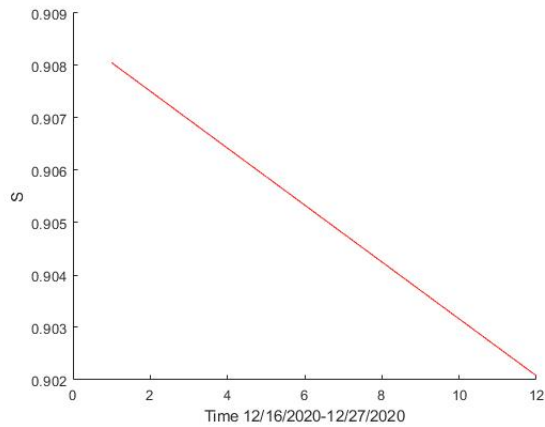


Figure 10:  $S$  from December 16 to December 22, 2020

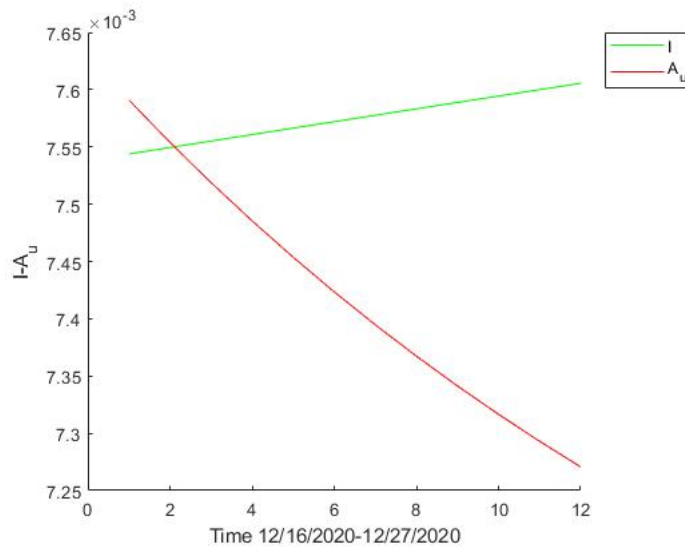


Figure 11:  $I$  and  $A_u$  from December 16 to December 22, 2020.

jump in vaccine administration at the end of the first week. The vaccine rollout plan, although targeted toward the higher-risk population, meant a longer wait until more vaccines became available. Those with underlying health conditions, people aged 65 and above, and first responders who received the vaccine during this time resulted in a slower vaccine administration in the first week. Although this helped the portion of susceptible people located in long-term care facilities, there was no significant effect on the susceptible population as a whole since the benefits of vaccination for the entire population could be reached with such a small vaccinated population [18]. Figure 11 shows the symptomatic

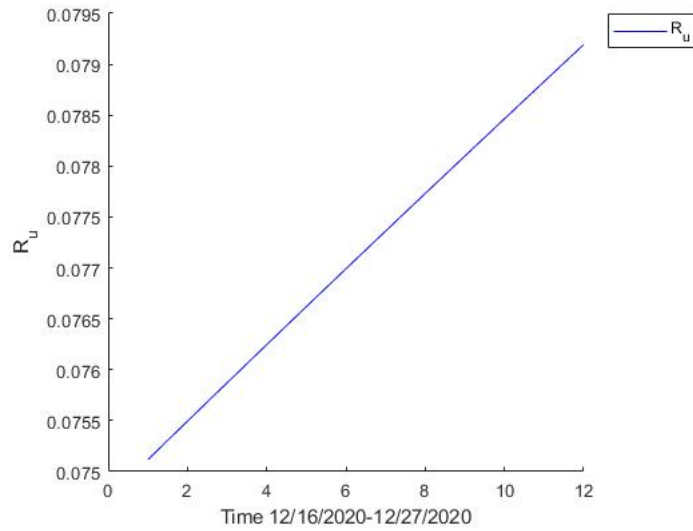


Figure 12:  $R_u$ , December 16 to December 22, 2020

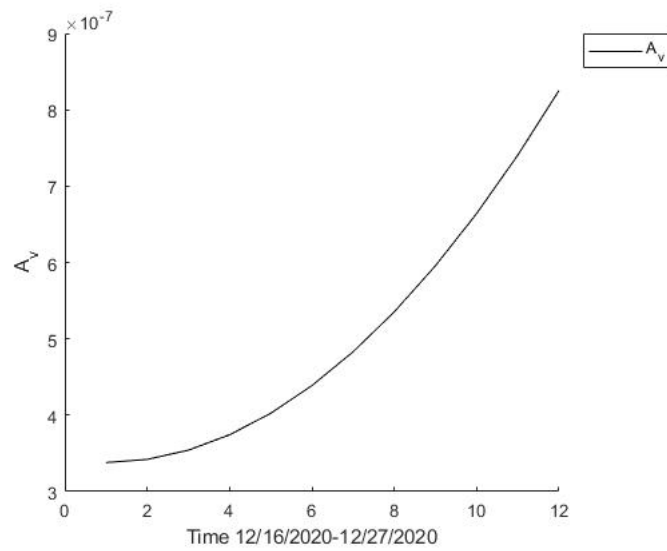


Figure 13:  $A_v$  from December 16 to December 22, 2020

This population accounts for those infected but received one dose of a vaccine.

infected population increased and the unvaccinated asymptomatic population decreased. Meanwhile, the unvaccinated recovered population continued to steadily grow as individuals recovered from the disease.

From Figures 13 and 14, those infected with one dose of the vaccine were not recovering within one week, resulting in a significantly smaller  $R_v$  population which can be regarded as 0. Due to the lower vaccine efficacy of an incomplete vaccine series, some

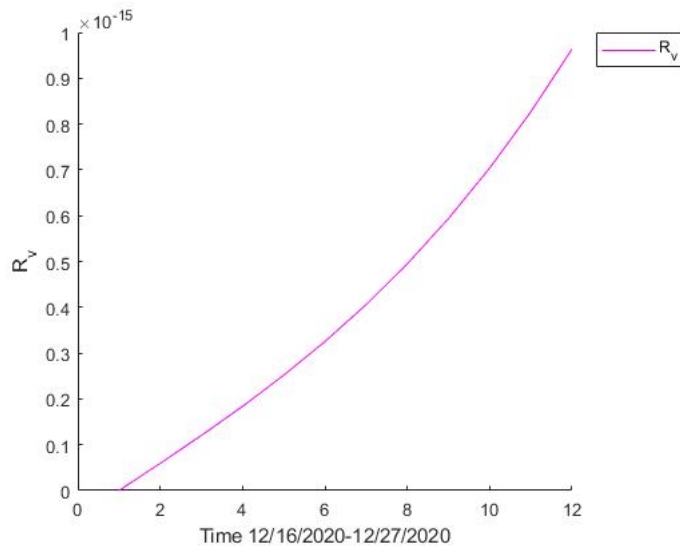


Figure 14:  $R_v$  from December 16 to December 22, 2020

breakthrough infections occurred within the vaccinated population. While the vaccinated population is still very small during this time, Figure 13 shows the steady but small increase in the vaccinated asymptomatic population with only one dose.

As with the previously observed time periods, the changes and reactions of the populations following the first week of vaccine administration caused the model to lose accuracy in the prediction of the next five days. The model required re-optimized parameters to account for these changes in the observed time periods.

One very interesting discovery from this set of parameters and initial conditions was the decrease of the unvaccinated asymptomatic population  $A_u$ . Figure 11 shows how, although the number of infected  $I$  was still slowly increasing, there was a drastic decrease in those with little to no symptoms. Since almost no data on the asymptomatic population exists, it is difficult to say if this is an accurate representation of the asymptomatic population.

Similarly, the time March 6, 2021 to March 20, 2021 was modeled with optimized parameters for 11 days from March 6, 2021 to March 16, 2021. Nearly a year after the first COVID-19 case in Mississippi and only a few months after the first vaccine administration, approximately 8% of the population was fully vaccinated. The data used to optimize the vaccination rate was collected from the CDC data on the total number of fully vaccinated



people [12]. The first collection of this data started on March 6, 2021. Similar to the time period with one dose of vaccines, the only initial conditions that are verifiable and accurate are the number of initial deceased individuals  $D(0)$  and the number of initial fully vaccinated individuals  $V(0)$ . As a weakness of our model, the number of initially infected individuals had to be approximated and assumed to obtain reasonable parameters. For this time period, we did not use the confirmed cases to approximate  $I(0)$  and instead included the value as a parameter to be optimized. This choice was made because of the model's weakness of using only the death and vaccine data since the model does not have a parameter to utilize other data sets such as confirmed cases. After some difficulty in approximating the initial conditions for the infected and recovered, the following initial conditions were used to optimize the parameters for this time period:

$$\begin{aligned}
I(0) &= 0.07416 & A_u(0) &= 0.0999 & A_v(0) &= 0.02 \times I(0) \\
D(0) &= 2.38817 \times 10^{-3} & R_u(0) &= 0.09708 & R_v(0) &= 0 \\
V(0) &= 0.08512 \\
S(0) &= 1 - (I(0) + A_u(0) + A_v(0) + R_u(0) + R_v(0) + D(0) + V(0))
\end{aligned} \tag{13}$$

The earliest recording from MDHS of cases coming from vaccinated individuals started in June. According to the MDHS, about 2% of cases came from those who were fully vaccinated for June, so we assumed the initial number of vaccinated but infected was 2% of the infected population on March 6, 2021. We expected to observe a change on March 16, 2021, when people ages 16 and above became eligible for the vaccine. The vaccine efficacy rate against the first major variant in the pandemic was established to be about 97% for those who are fully vaccinated, so  $\tau = 0.97$  [18]. The parameters were optimized to the following values:

$$\begin{aligned}
\alpha_I &= 0.8334 & \alpha_A &= 0.09796 & \xi &= 0.000016 \\
\rho_s &= 0.1183 & \rho_{Au} &= 0.10535 & \rho_{Av} &= 0.000134 \\
\mu &= 0.000047 & \nu &= 0.007118
\end{aligned} \tag{14}$$

Figures 15 through 21 display the spread of COVID-19 in Mississippi, albeit slower than the previously observed time period as the reproduction number was approximately

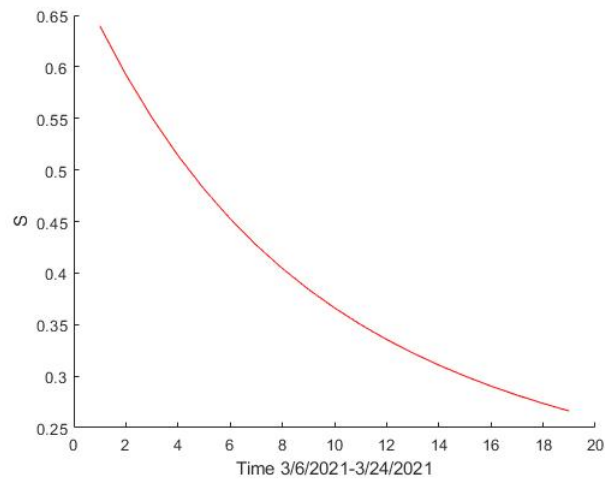


Figure 15:  $S$  from March 6 to March 24, 2021

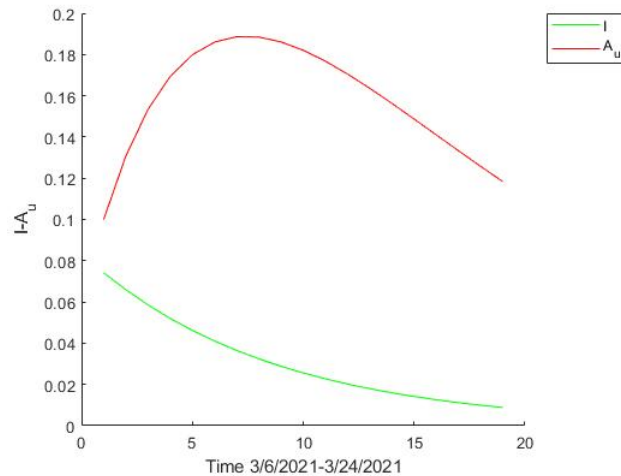


Figure 16:  $I$  and  $A_u$  from March 6 to March 24, 2021

In this figure, the number of infected is unrealistic by CDC data on confirmed cases.

2.45. Additionally, we predicted the last five days of this time period with the optimized parameters. These figures show unrealistic responses as verified by the CDC data on the daily confirmed cases. Figure 15 shows a drastic and unrealistic decline in the susceptible population while Figure 16 shows a high number of unvaccinated infected individuals, which stemmed from the unrealistic initial infected value calculated by optimization as a parameter. While those infected with symptoms decreased in number gradually throughout time, the unvaccinated asymptomatic population increased until a certain point and then

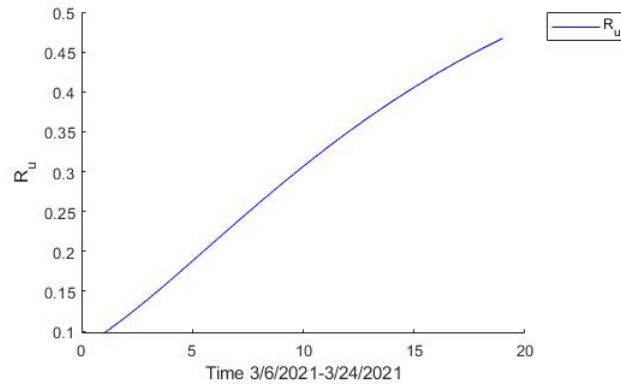


Figure 17:  $R_u$  from March 6 to March 24, 2021

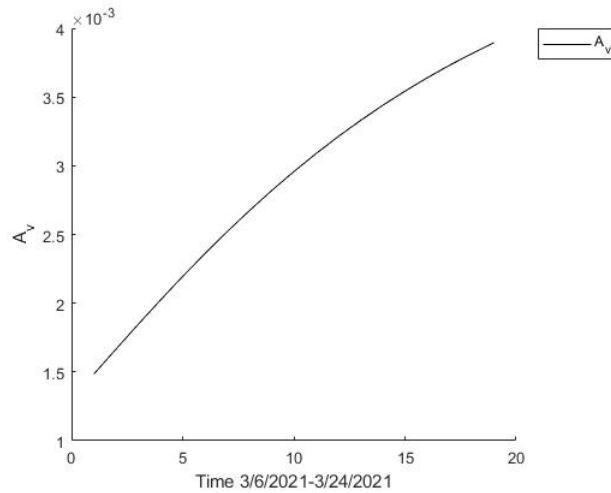


Figure 18:  $A_v$  from March 6 to March 24, 2021

decreased afterward for the rest of the twenty days. Since no data on the asymptomatic individuals was available due to a lack of testing and reporting, the  $A_u$  curve should not be considered accurate. Meanwhile, Figure 17 shows the drastic recovery of those who had been infected without being fully vaccinated. The vaccinated asymptomatic population was observed to increase from approximately 44,400 individuals to 118,000 individuals in 20 days.

Figures 20 and 21 show the parameter optimization for fully vaccinated individuals and deceased individuals respectively. While not a perfect fit, the vaccine compartment in Figure 20 shows the population size of fully vaccinated individuals did not meet the expectations of the model in twenty days with parameters optimized for the first 11 days. At

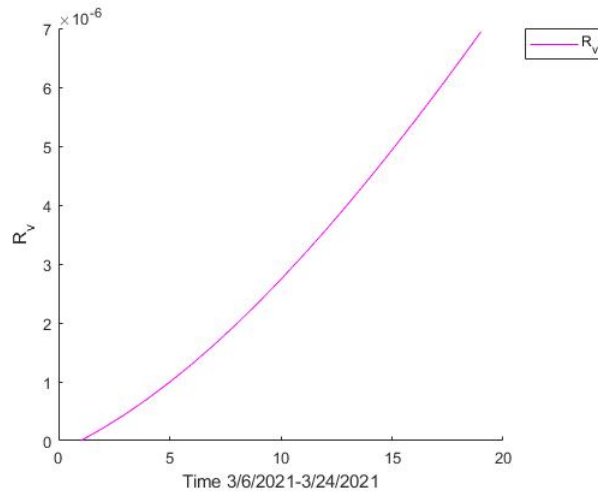


Figure 19:  $R_v$  from March 6 to March 24, 2021

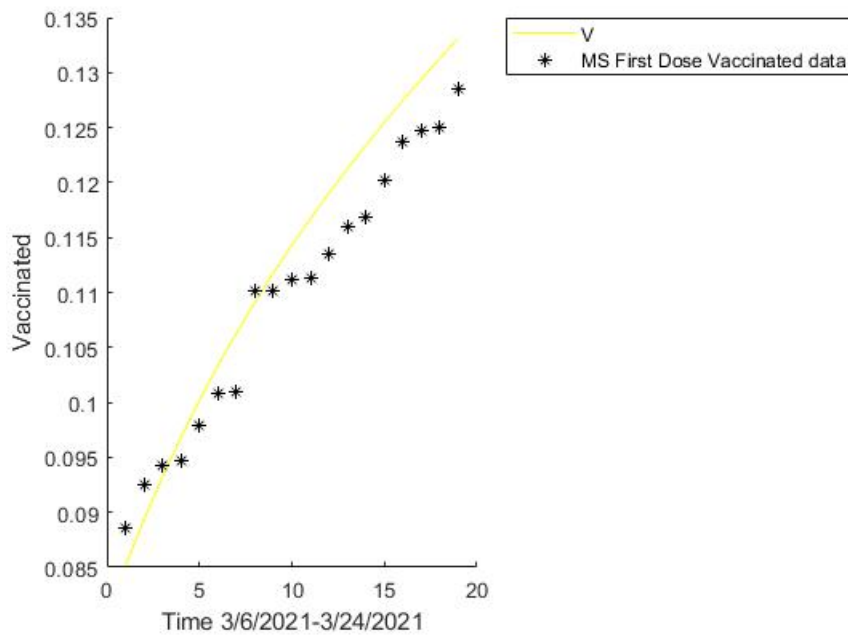


Figure 20: Data fitting  $V$  from March 6 to March 24, 2021

approximately March 16, the model no longer accurately represented the vaccine administration and deceased population in Mississippi. However, the data for vaccine administration was less than what the model predicted; with an expanse in eligible vaccinations, we would have expected the data to have values greater than the model predicted. However, since this change may be more gradual than anticipated, an expansion

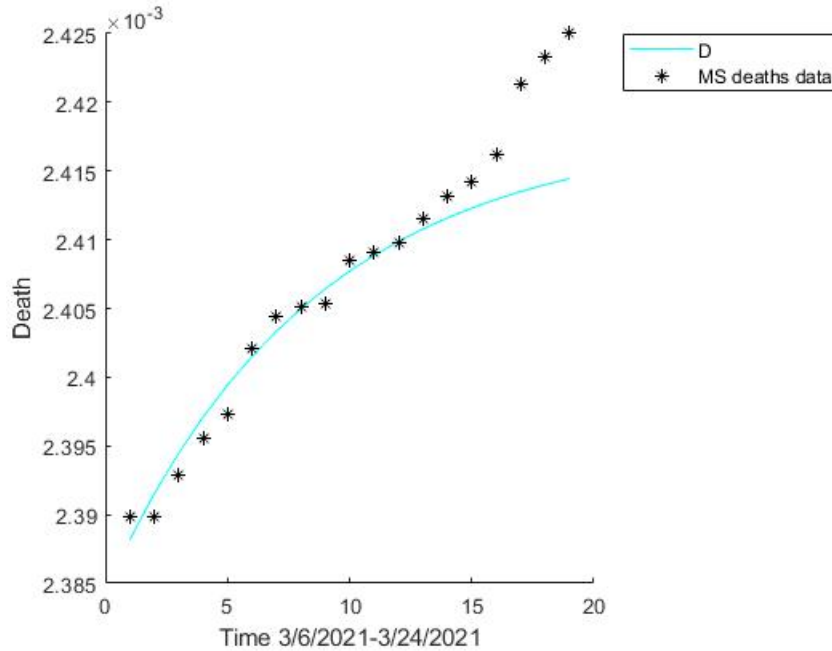


Figure 21: Data fitting for  $D$  from March 6 to March 24, 2021

of this time period would need to be optimized and simulated. Similarly, Figure 21 shows the data on deceased individuals did not agree with the predictions of the model for twenty days with parameters optimized for only 11 days. The lower vaccination rate was reflected in the death rate with an unexpected distance between the data values and the model values beginning after the tenth day observed for this period. We contemplated the possible reasons behind these unexpected changes in the next section. Lastly, since this time period has shown such unrealistic numbers of infected and recovered individuals, we do not claim these Figures represent the path of the pandemic in Mississippi during this time.

## CHAPTER V: CONCLUSION

In this study, we developed a simple epidemiological model to simulate the spread of COVID-19 in Mississippi with and without vaccinations. Due to the numerous changes in health policies and mandates that were declared as COVID-19 developed in Mississippi, our model created simulations for short periods of time. The daily confirmed case numbers, cumulative deceased, and cumulative vaccinated data were used to provide optimized parameters for these time periods; as seen in our results, these parameters in the model could not be accurately predicted without re-optimization for the next time period. In addition, a weakness of our model appeared when simulating for time periods further into the pandemic. Despite these shortcomings, we observed the effects of different health policies on the spread of COVID-19 in Mississippi by the changes that occurred between the model predictions and the available death and vaccine data.

Our results have shown interesting parameter values as well as some unexpected developments. During the period without the vaccine, March 4 to April 4, 2020, Figures 2 through 7 show the increased spread of COVID-19 in the population of Mississippi. The reproduction number  $\mathcal{R}_0$  in the model increased from 1.35 to 2.7 during this time, as well as the symptomatic infection rate  $\alpha_I$  from 0.00587 to 0.9646. Despite these increases, the strict health policies placed by Governor Tate Reeves helped decrease the death rate  $\mu$  from 0.0981 to 0.0764 between March 4 to March 23 and March 23 to April 4. Although the deaths were still increasing, the rate of deaths is observed to slow when comparing Figure 4 and Figure 7, where the optimized parameters forecasted more deaths than what the data shows. The asymptomatic infection rate  $\alpha_A$  also decreased from 1.62 to 0.3328 between these two time periods. The dramatic increase of asymptomatic individuals  $A_u$  is likely observed due to the probability of becoming asymptomatic  $(1 - \xi)$  increasing from 0.227 to 0.8462 between these two time periods. This could be caused by the increased infectiousness of the disease as well as the lack of testing in general. A lack of testing would increase the uncertainty that those who only show mild symptoms would not report or be tested. This uncertainty included in our model helped us understand the increase of

the basic reproduction number  $\mathcal{R}_0$  and the decrease in the death rate  $\mu$ .

Since we do not have available data on the number of asymptomatic cases, our conclusion should not be considered entirely accurate. In addition to those health policies, the decrease in the death rate and the asymptomatic infection rate was likely caused by the increased awareness of the disease, better information on treatments of the disease, and the number of individuals following health protocols.

In March of 2020, pharmaceutical companies Pfizer and BioNTech began the rapid development of COVID-19 vaccines; within nine months, vaccines were ready to be administered to the public. Two mRNA vaccines, Pfizer and Moderna, require two doses to be considered fully vaccinated at about 90% efficacy [17]. The Janssen vaccine requires one dose, but it is less effective than the mRNA vaccines, reporting only 66% efficacy two weeks after vaccination [20]. In this study, we observed the time of the first week of vaccine administration in Mississippi, December 16 to December 22, 2020, and the time of the first data available for fully vaccinated individuals, March 6 to March 24, 2021. Note that in the first week of vaccine administration observed, Janssen vaccines were not administered. Our results showed insightful parameter values and simulated, with predictions, the pandemic in Mississippi with vaccine administration.

Figures 8 through 21 show how vaccine administration was more gradual at preventing infection of COVID-19 in Mississippi than other preventions such as the Stay at Home order or mask mandates by observing the differences in the vaccine and death data and the solutions for compartments that the system computed. Despite the unrealistic responses as seen in the last time period observed, we observed the effects of different policies on the population. The reproduction number  $\mathcal{R}_0$  in the model decreased from 3.15 to 2.45, and the death rate  $\mu$  decreased from 0.001695 to 0.00005 between these two time periods. Despite these decreases, both the symptomatic infection rate  $\alpha_I$  and the asymptomatic infection rate  $\alpha_A$  increased from 0.0509 and 0.001625 to 0.8335 and 0.0979, respectively. This could be due to the high infectiousness of the disease while the vaccines were being administered, and it is not until individuals were becoming fully vaccinated that we observed a decrease in

the reproduction number. Note that the first observation of vaccine administration is the first week of vaccine administration in Mississippi. The low recovery rates were likely explained by people with severe symptoms not recovering within one week. In addition, the vaccination rate only accounted for those ages 65 and older and those with underlying health conditions; the vaccine efficacy for only one dose was found to be below 90% for all three types of vaccines [17] [20]. With a chosen efficacy rate of only 89% and a small portion of the susceptible population taking the vaccine, vaccine control measures had little effect on the number of deaths and infections in only one week. This is observed in Figures 8, 9, and 11, which forecasted as many deaths as the CDC data revealed.

Meanwhile, the model for the fully vaccinated individuals observed a different effect in Figures 15 to 21. By March 6, 2021, about 8% of the susceptible population in Mississippi was fully vaccinated. Figure 20 shows that the system did not model vaccine administration accurately after the ninth day; there were fewer vaccines administered than the system predicted. Similarly, Figure 21 predicted far fewer deaths than the CDC data revealed. Other figures during this time period also showed unrealistic infection and recovery populations. On March 16, all ages 16 and above became eligible for the vaccine; however, it takes more time for these additional people to be vaccinated if they so choose. Unlike mask mandates and the Executive Stay At Home Order, this vaccine administration only resulted in gradual changes to the spread of COVID-19 in Mississippi. In addition, a hesitancy to receive the vaccine emerged in Mississippi as social and political factors influenced the public perspective on vaccine safety. This combination of hesitancy and vaccine administration processes was a likely cause of the low total fully vaccinated population and slow vaccination rate, as well as the distance between the simulation and the CDC vaccine data. A few days before the observed time period, the mask mandates for all counties were lifted on March 2, 2021; masks were then only required in schools and when social distancing was not possible [22]. Observing Figure 16, this policy change could be the likely cause of the increase in asymptomatic individuals since those without symptoms are less likely to wear a mask in public. If the symptomatic individual population was on a



decline before this observed time period, the decreasing number of infected individuals may have spurred the lifted mask mandate.

The time periods observed for this study collectively demonstrated the importance of following recommended health guidelines and efficient vaccine administration. Only a limited number of people could be vaccinated at a time due to the hindrance of lines, wait times, and the number of available vaccines at a given location. More time was needed to administer vaccines to the entire susceptible population than each individual taking direct and immediate action themselves to slow the spread of COVID-19 in Mississippi. As a short-term solution, social distancing and staying at home were immediate actions that each susceptible individual could take at any given moment, restricting the spread more efficiently than the initial vaccine administration. In addition, when the vaccine had yet to be developed, these individual actions slowed the spread of the disease compared to what the system predicted. Only when more vaccines were made available for a larger part of the susceptible population did the vaccine administration prevent the spread of COVID-19 more effectively than the preventions observed during the first week. Once a larger percentage of the population has been vaccinated, we hope to observe a more controlled pandemic in Mississippi.

Throughout our research, several new insights into the COVID-19 disease changed the way we understand its infectiousness and spread across Mississippi. In addition, we learned about the unfortunate hospitalizations and deaths of those who received their full dose of a vaccine. These were caused by the more infectious variants that mutated from the original virus. The Delta variant in the summer of 2021 and the Omicron variant in the winter of 2021 both contributed greatly to rising cases and deaths. These developments compelled us to consider future improvement and research for our system of ordinary differential equations.

### **Future Research**

With the difficulties in developing an accurate model for the time period with vaccines,

several key improvements can be attained in the model. First, the model should use the initial number of infected people from an estimation by the number of confirmed cases. This would ensure some better, if not realistic, results for the fourth experiment tested by the *ASIRD – V* model. Limited time prevented this improvement in the model and the requisite code from being developed. The unrealistic values in the fourth experiment were used as an opportunity to learn where some faults in the model occurred. With more time and research, we could make significant improvements to the *ASIRD – V* model.

Additional research would include modifying the model for longer time periods, which may include developing a continuous function by which the parameters can account for changes in policy and vaccination administrations. Such a function was seen in [23] and could help expand the time period by which the model could reliably simulate. In addition, if looking to expand the time for which the model can simulate, then the model could be modified to include those individuals who become reinfected after recovery.

With these modifications, the model could be used to observe the effects of the control measures, such as health policies and vaccinations, for other variants of COVID-19 that have spread in Mississippi. Many variants of COVID-19 have shown to decrease the efficacy of the vaccines [4]. Beginning with the Delta variant, the model could compare the reproduction number of the spread of the Delta variant to the original variant and even the Omicron variant. New research has shown that those with the vaccine, either one dose or fully vaccinated, have a possibility of having severe symptoms, including death. Data has recently been gathered for those with and without the vaccine becoming hospitalized. With this new information, the *ASIRD – V* model could include a new compartment for those vaccinated and hospitalized with COVID-19, as well as new parameters to measure the rate of hospitalization and death for those vaccinated and infected with severe symptoms compared to those asymptomatic and vaccinated individuals.

## APPENDIX A: CODE

```

1 function [w,resnorm] = ASIRDVModel
2 format long
3 p=[.05,0.001,0.05,0.05,0.05,0,0.05,0];% %initial guess for ...
   optimization
4 lb=[0 0 0 0 0 0 0 0 ]; %lower bound;
5 ub=[50 5 5 5 5 5 5 5 ]; %upper bound;
6 options.StepTolerance = 1e-10;
7 options.FunctionTolerance=1e-10;
8
9 %from minimized cost function for t=20
10 [w,resnorm]= lsqnonlin(@myfun1,p,lb,ub,options)
11 MS=MSData; %MS death data and vaccine data
12
13 %parameters:alphaI-rate of I infection, alphaA-rate
14 %of asymptomatic (Au and Av) infection,
15 %xi-probability of becoming I, rhoS-recovery rate of I,
16 %rhoAu-recovery rate of Au
17 %rhoAv-recovery rate of Av, mu-death rate,
18 %nu-vaccination rate,
19 %tau-vacc. effectiveness
20 p= w;
21 alphaI=p(1);alphaA=p(2); xi=p(3);rhoS=p(4);
22 rhoAu=p(5); rhoAv=p(6); mu=p(7); nu=p(8); tau=0;
23 p=[ alphaI,alphaA, xi,rhoS,rhoAu, rhoAv, mu, nu, tau];
24
25 %initial conditions unified as proportion of total pop. of MS N=1
26 %(2,961,279) in 2020 0.19199e-3
27 I0=1.35e-6; Au0=1.24e-6;Av0=0; Ru0=0; Rv0=0; D0=0; V0=0;
28 S0=1-(I0+Au0+Av0+Ru0+Rv0+D0+V0);
29 options = odeset('RelTol',1e-4,'AbsTol',[1e-10 1e-10 1e-10
30 1e-10 1e-10 1e-10 1e-10]);
31 %time interval from data [3/4/20-3/24/20: first 20 days in data]
32 T0=MS(1:29,1);
33 Y0=[S0,I0,Au0,Av0,Ru0,Rv0,D0,V0]; %initial value
34 [T,Y]= ode45(@ (t,y)ASIRDV(t,y,p),T0,Y0,options);
35
36 %reproduction number
37 r0=(((1-xi)*S0*alphaA)/(rhoAu))+
38 (((1-tau)*V0*alphaA)/(rhoAv))+((xi*S0*alphaI)/(rhoS+mu))
39
40 %plot against death data
41 figure(3) %plots solution of D(t)
42 hold on %holds previous plots; doesnt replace previous graphs
43 plot(T,Y(:,7),'c-') %plots solution curve red dots
44 DD=MSData; %edit for death data
45 plot(DD(1:29,1),DD(1:29,2)/(2.96*10^6),'k*')
46 ylabel('Death')
47 xlabel('Time (days)3/25-4/16')
48 legend('D', 'MS deaths data','Location','NorthEastOutside')

```

```

49
50 %plot against vaccine data
51 figure(4)
52 hold on
53 plot(T,Y(:,8),'y-')
54 VV=MSData;
55 plot(VV(1:29,1),VV(1:29,8)/(2.96*10^6),'k*')
56 ylabel('Vaccinated')
57 xlabel('Time (days) 3/25-4/16')
58 legend('V','MS Fully Vaccinated data','Location','NorthEastOutside')
59
60 %plots solution of I,Au,Av,Ru,Rv,D,V
61 figure(1)
62 hold on
63 %plots solution curve
64 plot(T,Y(:,2),'g-',T,Y(:,3),'r-',T,Y(:,4),'k-',...
65      T,Y(:,5),'b-',T,Y(:,6),'m-',T,Y(:,7),'c-')
66 ylabel('I-A_u-A_v-R_u-R_v-D-V')
67 xlabel('Time 3/4/2020-4/1/2020')
68 legend('I','A_u','A_v','R_u','R_v','D','Location',...
        'NorthEastOutside')
69
70 %plot solution of Ru
71 %figure(5)
72 %hold on
73 %plot(T,Y(:,5),'b-')
74 %ylabel('Ru')
75 %xlabel('Time 3/4/2020-4/1/2020')
76 %legend('Ru','Location','NorthEastOutside')
77
78 %plots solution of S
79 figure(2)
80 hold on
81 plot(T,Y(:,1),'r-')
82 ylabel('Susceptible')
83 xlabel('Time 3/4/2020-4/1/2020')
84
85 %optimize parameters
86 function [F]= myfun1(p) %uncontrolled epidemic phase (up to t=20)
87     format long
88 MS=MSData; %MS data
89 q=[p,0];
90
91 I0=1.35e-6; Au0=1.24e-6;Av0=0; Ru0=0;
92 Rv0=0; D0=0; V0=0; S0=1-(I0+Au0+Av0+Ru0+Rv0+D0+V0);
93 options = odeset('RelTol',1e-4,'AbsTol',[1e-10 1e-10 1e-10 1e-10 ...
94                1e-10 1e-10 1e-10 1e-10]);
95 T0=MS(1:20,1); %time interval from data
96 Y0=[S0,I0,Au0,Av0,Ru0,Rv0,D0,V0]; %initial value
97
98 [T,Y]= ode45(@(t,y)ASIRDV(t,y,q),T0,Y0,options);
99
100 F= ((MS(1:20,2)/(2.96*10^6)-Y(T0,7))*(2.96*10^6))...
    +((MS(1:20,8)/(2.96*10^6)-Y(T0,8))*(2.96*10^6));

```

```

101
102 %solve system
103 function dy=ASIRDV(t,y,p) %nonlin ODE system function
104     format long
105     dy= zeros(8,1); %vector of 0
106     alphaI=p(1); alphaA=p(2); xi=p(3); rhoS=p(4); rhoAu=p(5);
107     rhoAv=0;mu=p(7); nu=0; tau=0;%parameter list
108     dy(1)=-y(1)*(alphaI*y(2)+alphaA*y(3)+alphaA*y(4))-nu*y(1);
109     dy(2)=xi*y(1)*(alphaI*y(2)+alphaA*y(3)+alphaA*y(4))-(rhoS ...
110         +mu)*y(2);
111     dy(3)=(1-xi)*y(1)*(alphaI*y(2)+alphaA*y(3)+alphaA*y(4)) ...
112         -rhoAu*y(3);
113     dy(4)=(1-tau)*y(8)*(alphaI*y(2)+alphaA*y(3)+alphaA*y(4)) ...
114         -rhoAv*y(4);
115     dy(5)=rhoS*y(2)+rhoAu*y(3);
116     dy(6)=rhoAv*y(4);
117     dy(7)=mu*y(2);
118     dy(8)=nu*y(1)-(1-tau)*y(8)*(alphaI*y(2)+alphaA*y(3) ...
119         +alphaA*y(4));

```

## APPENDIX B: DATA

All data is downloaded from the CDC website [12][13].

*Table B.1: March 4 to March 23, 2020*

\*Total doses for Janssen, Moderna and Pfizer vaccines

| Day | Confirmed Deaths | Total Administered Vaccines | J* | M* | P* | New Cases | Fully Vaccinated | Confirmed Cases |
|-----|------------------|-----------------------------|----|----|----|-----------|------------------|-----------------|
| 1   | 0                | 0                           | 0  | 0  | 0  | 6         | 0                | 4               |
| 2   | 1                | 0                           | 0  | 0  | 0  | 2         | 0                | 5               |
| 3   | 2                | 0                           | 0  | 0  | 0  | 12        | 0                | 16              |
| 4   | 2                | 0                           | 0  | 0  | 0  | 8         | 0                | 24              |
| 5   | 4                | 0                           | 0  | 0  | 0  | 11        | 0                | 35              |
| 6   | 5                | 0                           | 0  | 0  | 0  | 35        | 0                | 70              |
| 7   | 6                | 0                           | 0  | 0  | 0  | 25        | 0                | 94              |
| 8   | 11               | 0                           | 0  | 0  | 0  | 23        | 0                | 117             |
| 9   | 13               | 0                           | 0  | 0  | 0  | 35        | 0                | 153             |
| 10  | 15               | 0                           | 0  | 0  | 0  | 37        | 0                | 189             |
| 11  | 23               | 0                           | 0  | 0  | 0  | 41        | 0                | 230             |
| 12  | 28               | 0                           | 0  | 0  | 0  | 71        | 0                | 300             |
| 13  | 37               | 0                           | 0  | 0  | 0  | 96        | 0                | 391             |
| 14  | 43               | 0                           | 0  | 0  | 0  | 80        | 0                | 469             |
| 15  | 53               | 0                           | 0  | 0  | 0  | 112       | 0                | 580             |
| 16  | 59               | 0                           | 0  | 0  | 0  | 95        | 0                | 674             |
| 17  | 70               | 0                           | 0  | 0  | 0  | 125       | 0                | 797             |
| 18  | 78               | 0                           | 0  | 0  | 0  | 98        | 0                | 894             |
| 19  | 83               | 0                           | 0  | 0  | 0  | 92        | 0                | 986             |
| 20  | 86               | 0                           | 0  | 0  | 0  | 165       | 0                | 1151            |

Table B.2: March 23 to April 1, 2020

\*Total doses for Janssen, Moderna, and Pfizer vaccines

| Day | Confirmed Deaths | Total Administered Vaccines | J* | M* | P* | New Cases | Fully Vaccinated | Confirmed Cases |
|-----|------------------|-----------------------------|----|----|----|-----------|------------------|-----------------|
| 20  | 86               | 0                           | 0  | 0  | 0  | 165       | 0                | 1151            |
| 21  | 93               | 0                           | 0  | 0  | 0  | 138       | 0                | 1288            |
| 22  | 102              | 0                           | 0  | 0  | 0  | 132       | 0                | 1420            |
| 23  | 109              | 0                           | 0  | 0  | 0  | 120       | 0                | 1540            |
| 24  | 117              | 0                           | 0  | 0  | 0  | 165       | 0                | 1705            |
| 25  | 121              | 0                           | 0  | 0  | 0  | 102       | 0                | 1807            |
| 26  | 128              | 0                           | 0  | 0  | 0  | 102       | 0                | 1909            |
| 27  | 139              | 0                           | 0  | 0  | 0  | 163       | 0                | 2071            |
| 28  | 153              | 0                           | 0  | 0  | 0  | 151       | 0                | 2222            |
| 29  | 164              | 0                           | 0  | 0  | 0  | 154       | 0                | 2374            |

Table B.3: December 16 to December 22, 2020

| Day | Confirmed Deaths | Total Administered Vaccines | Janssen | Moderna |
|-----|------------------|-----------------------------|---------|---------|
| 288 | 5013             | 5                           | 0       | 0       |
| 289 | 5049             | 74                          | 0       | 1       |
| 290 | 5084             | 511                         | 0       | 1       |
| 291 | 5116             | 1497                        | 0       | 2       |
| 292 | 5141             | 2697                        | 0       | 2       |
| 293 | 5193             | 2975                        | 0       | 2       |
| 294 | 5230             | 3094                        | 0       | 2       |

| Day | Pfizer | New Cases | Fully Vaccinated | Confirmed Cases |
|-----|--------|-----------|------------------|-----------------|
| 288 | 5      | 2156      | 0                | 191002          |
| 289 | 73     | 2083      | 0                | 193085          |
| 290 | 509    | 2154      | 0                | 195239          |
| 291 | 1494   | 1972      | 0                | 197211          |
| 292 | 2663   | 1099      | 0                | 198310          |
| 293 | 2941   | 2160      | 0                | 200470          |
| 294 | 3060   | 2223      | 0                | 202693          |

Table B.4: March 6 to March 16, 2021

| Day | Confirmed Deaths | Total Administered Vaccines | Janssen | Moderna |
|-----|------------------|-----------------------------|---------|---------|
| 368 | 7074             | 736826                      | 2099    | 401465  |
| 369 | 7074             | 764699                      | 4728    | 415493  |
| 370 | 7083             | 776272                      | 5325    | 417809  |
| 371 | 7091             | 780649                      | 5473    | 418511  |
| 372 | 7096             | 801306                      | 8485    | 428259  |
| 373 | 7110             | 823604                      | 10876   | 439637  |
| 374 | 7117             | 824528                      | 10877   | 440406  |
| 375 | 7119             | 896984                      | 16911   | 477742  |
| 376 | 7120             | 896984                      | 16911   | 477742  |
| 377 | 7129             | 904066                      | 17446   | 480404  |
| 378 | 7131             | 906140                      | 17525   | 481112  |

| Day | Pfizer | New Cases | Fully Vaccinated | Confirmed Cases |
|-----|--------|-----------|------------------|-----------------|
| 368 | 332965 | 201       | 262010           | 298946          |
| 369 | 344100 | 156       | 273824           | 299102          |
| 370 | 352744 | 433       | 278797           | 299535          |
| 371 | 356271 | 457       | 280373           | 299992          |
| 372 | 364099 | 511       | 289830           | 300503          |
| 373 | 372596 | 656       | 298373           | 301159          |
| 374 | 372750 | 395       | 298916           | 301554          |
| 375 | 401756 | 201       | 326150           | 301755          |
| 376 | 401756 | 156       | 326212           | 301911          |
| 377 | 405641 | 418       | 329254           | 302329          |
| 378 | 406928 | 283       | 329647           | 302612          |



## REFERENCES

- [1] Kermack W. & McKendrick A.G. A contribution to the mathematical theory of epidemics. August 1, 1927. Proceedings of the Royal Society. Mathematical, Physical and Engineering Sciences. <https://doi.org/10.1098/rspa.1927.0118>
- [2] Abdy M., Side S., Annas S., et al. An SIR epidemic model for COVID-19 spread with fuzzy parameter: the case of Indonesia. *Advances in Difference Equations* 2021;105. <https://doi.org/10.1186/s13662-021-03263-6>
- [3] Krivorot'ko O.I., Kabanikhin S.I., Zyat'kov N. Y., et al. Mathematical Modeling and Forecasting of COVID-19 in Moscow and Novosibirsk Region. *Numerical Analysis and Applications* 2020; 13(4):332-348. DOI: 10.1134/S1995423920040047
- [4] Lopez Bernal J., Andrews N., Gower C., et. al. Effectiveness of Covid-19 Vaccines against the B.1.617.2 (Delta) Variant. *The New England Journal of Medicine* 2021;385(7):585-594.
- [5] Ramos A.M., Ferrández M.R., Vela-Pérez M., et al. A simple but complex enough  $\theta$ -SIR type model to be used with COVID-19 real data. Application to the case of Italy. *Physica D* 2021;421(132839).
- [6] Driessche P. & Watmough J., Further Notes on the Basic Reproduction Number 2008. DOI:10.1007/978-3-540-78911-6\_6
- [7] De la Sen M. & Ibeas A. On an SE(Is)(Ih)AR epidemic model with combined vaccination and antiviral controls for COVID-19 pandemic. *Advances in Difference Equations* 2021;92(2021) <https://doi.org/10.1186/s13662-021-03248-5>
- [8] Zhang T. Permanence and extinction in a nonautonomous discrete SIRVS epidemic model with vaccination. *Applied Mathematics and Computation* 2015;271:716-729. <https://doi.org/10.1016/j.amc.2015.09.071>
- [9] Olivares A. & Staffetti E. Uncertainty quantification of a mathematical model of COVID-19 transmission dynamics with mass vaccination strategy. *Chaos, Solitons and Fractals* 2021;146(110895). <https://doi.org/10.1016/j.chaos.2021.110895>
- [10] Ramos A.M., Ferrández M.R., Vela-Pérez M., et al. Modeling the impact of SARS-CoV-2 variants and vaccines on the spread of COVID-19. *Commun Nonlinear Sci Numer Simulat* 2021;102(105937). <https://doi.org/10.1016/j.cnsns.2021.105937>.
- [11] Bachar M., Khamsi M., & Bounkhel M. A mathematical model for the spread of COVID-19 and control mechanisms in Saudi Arabia. *Advances in Difference Equations* 2021;253. <https://doi.org/10.1186/s13662-021-03410-z>
- [12] NCIRD. COVID-19 Vaccinations in the United States, Jurisdiction 2021. Centers for Disease Control. <https://data.cdc.gov/Vaccinations/COVID-19-Vaccinations-in-the-United-States-Jurisdi/unsk-b7fc>

- [13] Surveillance Review and Response Group. United States COVID-19 Cases and Deaths by State over Time 2020. Centers for Disease Control. <https://data.cdc.gov/Case-Surveillance/United-States-COVID-19-Cases-and-Deaths-by-State-o/9mfq-cb36>.
- [14] Tchoumi S.Y., Diagne M.L., Rwezaura H. & Tchuenche J.M. Malaria and COVID-19 co-dynamics: A mathematical model and optimal control. *Applied Mathematical Modeling* 2021;99:294-327. DOI: <https://doi.org/10.1016/j.apm.2021.06.016>
- [15] Otoo D., Donkoh E.K. & Kessie J.A. Estimating the basic reproductive number of COVID-19 cases in Ghana. *European Journal of Pure and Applied Mathematics* 2021;14(1):135-148.
- [16] Panella A. & Sickinger M. Modeling the spread of the COVID-19 in Mississippi with the ASIRD model. Wright W. and Annie Rea Cross Mathematics Undergraduate Research Program, The University of Southern Mississippi. July 2021. [PowerPoint].
- [17] Fowlkes A., Gaglani M., Groover K., et al. Effectiveness of COVID-19 vaccines in preventing SARS-CoV-2 infection among frontline workers before and during B.1.617.2 (Delta) variant predominance-Eight U.S. Locations, December 2020-August 2021. *MMWR Morbidity and Mortality Weekly Report* 2021;70:1167-1169. DOI: <http://dx.doi.org/10.15585/mmwr.mm7034e4>
- [18] Nanduri S., Pilishvili T., Derado G., et al. Effectiveness of Pfizer-BioNTech and Moderna vaccines in preventing SARS-CoV-2 infection among nursing home residents before and during widespread circulation of the SARS-CoV-2 B.1.617.2 (Delta) variant- National Healthcare Safety Network, March 1-August 1, 2021. *MMWR Morbidity and Mortality Weekly Report* 2021;70:1163-1166. DOI: <http://dx.doi.org/10.15585/mmwr.mm7034e3>
- [19] Centers for Disease Control. Delta Variant: What we know about the science. NCIRD, Division of Viral Diseases. August 26, 2021. <https://www.cdc.gov/coronavirus/2019-ncov/variants/delta-variant.html>
- [20] Oliver S.E., Gargano J.W., Scobie H., et al. The Advisory Committee on Immunization Practices' Interim Recommendation for Use of Janssen COVID-19 Vaccine-United States, February 2021. *MMWR Morbidity and Mortality Weekly Report* 2021;70:329-332. DOI: <http://dx.doi.org/10.15585/mmwr.mm7009e4>
- [21] MSDH. COVID-19 Cases by Variants of Concern and Date Collection, Mississippi, January 1-September 20, 2021. Mississippi State Department of Health. [https://msdh.ms.gov/msdhsite/index.cfm/14,13324,420,pdf/COVID-19\\_Cases\\_by\\_Variant\\_Type.pdf](https://msdh.ms.gov/msdhsite/index.cfm/14,13324,420,pdf/COVID-19_Cases_by_Variant_Type.pdf)
- [22] Watson, Micheal. Executive Orders. 2021. Mississippi Secretary of State. <https://www.sos.ms.gov/communications-publications/executive-orders>
- [23] Neves A. & Guerrero G. Predicting the evolution of the COVID-19 epidemic with the A-SIR model: Lombardy, Italy and São Paulo state, Brazil, *Physica D* 2020; 413. DOI: <https://doi.org/10.1016/j.physd.2020.132693>

- [24] Aziz-Alaoui M.A., Najm F. & Yafia R. SIARD model and effect of lockdown on the dynamics of COVID-19 disease with non total immunity. *Mathematical Modeling of Natural Phenomena* 2021;16(31). DOI: <https://doi.org/10.1051/mmnp/2021025>
- [25] Hongfan L., Ding Y., Gong S. & Wang S. Mathematical modeling and dynamic analysis of SIQR model with delay for pandemic COVID-19. *Mathematical Biosciences and Engineering* 2021; 18(4):3197-3214. DOI: [10.3934/mbe.2021159](https://doi.org/10.3934/mbe.2021159)
- [26] Ritchie H., Mathieu E., Rodés-Guirao L., et al. "Coronavirus Pandemic (COVID-19)". 2020. Published online at [OurWorldInData.org](https://ourworldindata.org/coronavirus). <https://ourworldindata.org/coronavirus>